Study programme:

Biology

Branch of study:

Cellular and molecular biology of plants

Bc. Viktoria D'Agostino

Comparative phenotypic study of selected Arabidopsis formin mutants

Diploma thesis

Supervisor:

doc.RNDr. Fatima Cvrčková, Dr.

Prague 2018

Prohlášení:

Prohlašuji, že jsem závěrečnou práci zpracovala samostatně a že jsem uvedla všechny použité informační zdroje a literaturu. Tato práce ani její podstatná část nebyla předložena k získání jiného nebo stejného akademického titulu.

V Praze, 13.8.2018

Abstract

Actin filaments and microtubules are involved in cell development and morphogenesis. Plant Class II formins regulate both cytoskeletal polymers. However their function has not yet been fully described. This study examines effects of LOF mutations in *Arabidopsis thaliana* FH13 (AT5G58160) and FH14 (AT1G31810) genes on early root system development using a pharmacological approach. Since measuring root length of numerous mutant lines in multiple conditions is laborious and time consuming, this thesis also involves optimization of this process with the aim to establish a reliable method of fast visualisation and measurement of *Arabidopsis* seedlings in a time series in the laboratory. Furthermore, statistical analysis for a large amount of data gathered in multiple conditions had to be optimized. While no significant phenotype in terms of root length was found in *fh13*, *fh14* and double *fh13 fh14* LOF mutants under standard conditions, treatment with cytoskeletal drugs revealed possible changes in lateral root branching in an *fh14* mutant. Nevertheless, specific function of FH13 and FH14 remains a question.

Abstrakt

Aktinová vlákna a mikrotubuly se podílejí na vývoji a tvaru buňky. Rostlinné forminy třídy II regulují oba typy cytoskeletárních polymerů. Nicméně jejich funkce zatím nebyla zcela popsána. Tato studie se zaměřuje na efekty ztrátových mutací v genech FH13 (AT5G58160) and FH14 (AT1G31810) *Arabidopsis thaliana*, konkrétně na vývoj kořenového systému s použitím farmakologických postupů. Vzhledem k tomu, že měření kořenů rostlin za různých podmínek je pracné a časově náročné, tato diplomová práce se také zaměřuje na optimalizaci tohoto procesu, s cílem vytvořit metodu rychlé vizualizace a měření růstu semenáčků *Arabidopsis* v laboratorních podmínkách. Kromě toho bylo též nutné optimalizovat statistickou analýzu pro velké množství dat shromážděných za různých typů podmínek. Zatímco za standartních podmínek nebyl nalezen statisticky významný fenotyp, co se týče délky kořenů mutantů *fh13*, *fh14* a dvojtého mutanta *fh13 fh14* působení cytoskeletárních drog odhalailo změny ve vzniku laterárních kořenů mutanta *fh14*. Nicméně specifická funkce FH13 a FH14 zůstává otázkou.

Table of Contents

List of abbreviations

AFs actin filaments
APC Adenomatous polyposis coli protein, nucleates actin
ARP2/3 Complex of Actin-related proteins 2 and 3
C2 domains take their name from the domain of protein kinase C that binds Ca^{2+}
Capu formin actin nucleator Cappuccino of Drosophila melanogaster
Cdc Cell-division cycle
CLIP170 microtubule-end-tracking protein
EB end binding protein, binds to microtubules
F-actin filamentous actin
FH formin homology
G-actin globular actin
GFP Green fluorescent protein
GOE Group Ie domain (found in AtFH4, AtFH7, AtFH8)
GTP/GDP Guanin nucleotide tris-/bisphosphate
LD limb deformation
mDia human/mouse homolog of Diaphanous in Drosophila
MTs mikrotubules
PCR Polymerase Chain Reaction
PTEN Phosphatase and tensin homolog deleted on chromosome ten
SMIFH2 formin FH2 inhibitor

Introduction

The admirable diversity of plant kingdom is based on great variability of forms. Final shape of each cell is carefully regulated by many factors. Some regions of the cell expand more, some less. Cytoskeleton, a complex structure within the cell, is one of the main factors of this process. Unequal expansion is apparent especially in cells undergoing rapid polarized growth such as pollen tubes, trichomes, root hairs and cell types with complex shape modulation like pavement cells of leaf epidermis. Not only does the cytoskeleton play a crucial role in morphogenesis, intracellular organisation, vesicular transport, cytokinesis, but also rapid movements such as stomata opening.

Actin dynamics

Actin in plants provides track for organelles and is responsible for well known phenomena such as plastid movement or cytoplasmic steaming, dynamics of endoplasmic reticulum (Sparkes et al., 2009) and Golgi apparatus (Nebenführ *et al.*, 1999). Actin network is a dynamic structure based on continuous assembly and disassembly (Pollard and Borisy, 2003). The balance between these two processes is regulated by the availability of free subunits in cytoplasm and by the presence of other accessory proteins. These are required for controlled polymerization, inhibition of growth or disassembly, nucleation and branching. The final F-actin network maintains the direction of vesicle deposition via actin-myosin and by creating either a loose sieve to let vesicles trough or a dense net which determines the release of proteins and polysaccharides to the cell wall and thus location of growth (Mathur, 2003a).

Actin nucleation

Globular actin (G-actin) units are able to assemble spontaneously to form dimers or trimers. However these “seeds” are unstable (Deeks and Hussey, 2003). Forming a stable actin filament requires additional proteins. There are several mechanisms known in eukaryotes, the best characterized being the ARP2/3 complex (Mathur, 2003b) and formins (Michelot, 2005).

Arp2/3 consists of seven subunits (Robinson, 2001). Two of these subunits Arp2 and Arp3, mimic actin subunits and by creating a “seed” within the complex they initiate polymerization of a new filament in the angle of exactly 70°*(*Blanchoin *et al.*, 2000). The

complex is bound to the filament at its pointed (-) end which is stabilized and polymerization occurs at the barbed (+) end (Pollard and Borisy, 2003). Loss of function in *Arabidopsis thaliana* causes accumulation of denser actin bundles and miss-localized cortical domains in trichomes (Le *et al.*, 2003), epidermal cells, hypocotyl cells and root hairs (Mathur, 2003a; Mathur, 2003b). However lack of functional Arp2/3 complex does not abolish actin nucleation completely suggesting an alternative nucleating mechanism.

Formins are second most abundant nucleators. They have been found in all eukaryotes and seem to have multiple functions. The process of formin triggered nucleation has not been sufficiently described in plants. It seems that formin travels along an existing actin filament and at a certain point triggers assembly of a new filament in an angle different to the one observed with Arp2/3 (Michelot, 2005). Unlike Arp2/3 complex, formins bind to the barbed end where they compete with polymerization inhibitor Capping protein (Michelot, 2005), allowing the filament to elongate slowly. Growth is accelerated by presence of Profilin protein providing G-actin to the barbed end (Pollard and Borisy, 2003). Above the nucleating function AFs form bundles in presence of formins (Michelot *et al.*, 2006).

Formin structure

First formin to be discovered was in *Mus musculus*. Mutation caused limb deformation (*ld* phenotype) and thus was thought to be responsible for limb formation, therefor the name Formin (Maas *et al.*, 1990). Later it was found that *ld* defects are not caused by disruption of Formin itself but by altered transcription of a neighbouring gene Gremlin. However the name remained (Zuniga, 2004). Soon a large number of genes have been found containing related sequences. They have been designated as members of the formin family.

Formin proteins are composed of several domains, which are present in different combinations and species-specific varieties (Grunt *et al.*, 2008). Determining feature of all formins is the FH2 (Formin homology 2) domain residing at C-terminus. Curiously it seems to be highly conserved in all eukaryotic organisms. FH2 forms a dimer (Xu *et al.*, 2004), binds actin and promotes actin nucleation *in vitro* (Pruyne, 2002). It slows down elongation and remains blocking the barbed end in a processive manner wobbling up as the filament grows. But when combined with other domains it gains

new functions. Typically, it is FH1 domain, which interacts with profilin and promotes filament growth. In budding yeast *Schizosaccharomyces cerevisiae* Bni1p protein bound to profilin is required for actin filament nucleation and assembly in vivo (Evangelista, 2003).

To explain formin-profilin interaction in detail, we have to take a closer look into the protein structure. FH1 domain contains a poly-L-proline sequence. Profilin is able to bind FH1 at this proline-rich structure but also binds G-actin (Chang, 1997) and can promote filament growth by delivering ATP-bound actin monomers to the growing barbed end (Theriot and Mitchison, 1993). For example, the formin Cdc12p is a crucial regulator of actin cortical ring during mitosis in *Schizosaccharomyces pombe*. Cdc12p can behave as a barbed-end capping protein with ability to decrease polymerization at this end. Cdc12p also generates filaments that then grow at their pointed ends. Profilin inhibits the activity of Cdc12p and thus allows the barbed-end to grow as fast as uncapped filaments (Kovar *et al.*, 2003).

While FH1 domain has a rather regulatory function, FH2 is responsible for F-actin assembly at the barbed end. Additional domains may contribute to redirecting the position of filament barbed ends to specific sites in the cell. For instance, the regulatory domain FH3 of mDia1 is responsible for localization to the mitotic spindle in HeLa cells (Kato *et al.*, 2001). FH3 overlaps with a regulatory domain activated by Rho GTPases also affecting the localization during cytokinesis (Higgs, 2005). GBD (GTPase binding domain) can be found in fungi and metazoans but not in vascular plants FH3 can be only found in plants with flagellate sperm (Grunt *et al.*, 2008; Cvrčková *et al.*, 2012)

Investigating plant formins is tricky because angiosperms have evolved many homologues. Amplification of formin genes is generally associated with plants expanding to dry land (Grunt *et al.*, 2008) allowing structural rearrangements and functional diversity within the formin family. It has been proposed that each diversification could be related to an evolutionary event (Cvrčková *et al.*, 2004). *Arabidopsis thaliana* has 21 formin genes divided into two classes (Figure 1) based on their protein structure. Class I typical structure begins with FH2 at C-terminus, FH1 and secretory signal sequence followed by a putative transmembrane domain at N-terminus. Class II also has FH2 and FH1 but is defined by PTEN-like domain at C`

terminus (Figure 1). The role of PTEN-like domain is unknown. PTEN (Phosphatase and tensin homolog) got the name after similar sequence found in beef phosphatase and chicken tensin (Li, 1997). It consists of two parts: lipid phosphatase and C2 domain. C2 domain possibly binds to membranes and vesicles. Animal C2 has a phosphatase activity (Maehama and Dixon, 1998) and prevents PTEN from binding to membrane. In plants however, bioinformatic analysis shows modification in sequence and thus phosphatase activity is no longer expected (Cvrčková *et al.*, 2004). Membrane binding has been reported in case of AtPTEN1. In moss *Physcomitrella patens* cortical localization is provided via interaction with phosphoinositide-3,5-bisphosphate at the membrane (van Gisbergen *et al.*, 2012) Whether class II formins have the ability to bind membranes in vascular plants is a question.

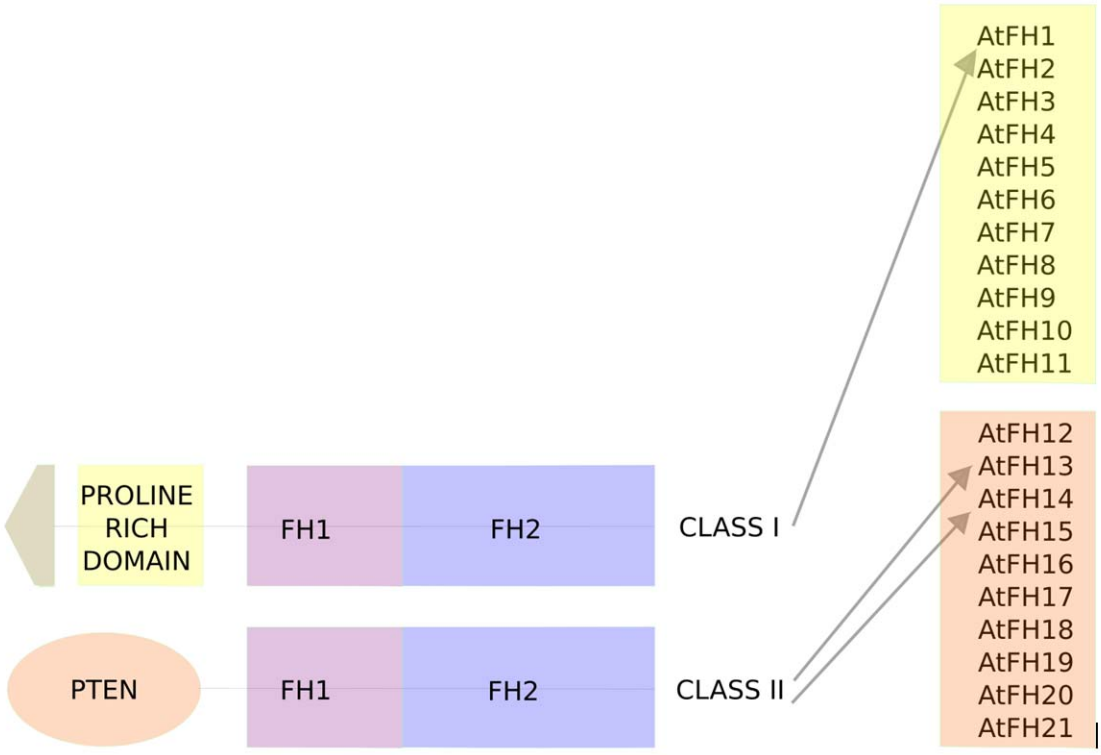

Figure 1. Schematic picture of protein structure typical for class I and Class II plant formins (Cvrčková *et al.*, 2004) in *Arabidopsis thaliana*.

In animal formin mDia2 and Capu FH2 domain also binds directly to microtubules mediating interaction between actin filaments and microtubules (Bartolini *et al.*,

2008;Rosales-Nieves *et al.*, 2006). Interaction can be also facilitated trough mediator proteins such as CLIP170, APC and EB1, which bind to the plus end of microtubules (Lewkowicz *et al.*, 2008;Wen *et al.*, 2004).

Microtubule interaction might also be mediated by other domains within the formin. In AtFh4 this has been resolved by the discovery of GOE domain (Deeks *et al.*, 2010). AtFh16, AtFh14, OsFh5 also have the ability to bind microtubules (Wang *et al.*, 2013), Whether the interaction is direct or mediated trough a linker protein is not yet been sufficiently explained.

Formin family members in plants

As mentioned before, plants have a large number of formin homologs. Several selected members of the formin family in *A. thaliana* shall be discussed now, comprising some interesting points, which I have considered as necessary to mention for further understanding of this work.

Class I formins

Formins numbered FH1 - 11 are known as Class I formins. Above FH1 and FH2 their structure in most cases contains a unique N' terminal structure with a secretory signal sequence, putative extracellular sequence and a trans-membrane domain. This structure seems to be plant-specific with the only few exceptions in protists and invertebrate metazoans (Grunt *et al.*, 2008). The membrane binding activity of FH1 (Cheung, 2004) and Atfh6 (Favery, 2004) has been observed *in vitro* and *in vivo*, and revealed function during tip growth and polarized expansion. Furthermore, FH1 anchors actin filaments to the cell wall (Martini *et al.*, 2011).

FH1

FH1 (or AtFH1 gene) is the most expressed class I formin in Arabidopsis and thus has been investigated the most in terms of function. So far it is known to have significant influence on both actin and microtubules. Fluorescently labelled actin polymerized in presence of AtFH1(Rosero *et al.*, 2013). At the origin of nucleation the number of

fluorescent impulses were compared with number of filaments growing from this point. It seems that AtFH1 can promote nucleation of multiple actin filaments. Quite possibly by working as a dimer or multimer. Fluorescent labelling showed that AtFH1 does not slide along the growing filament thus works nonprocessively. Unlike Arp2/3complex, AtFH1 acts at barbed ends of actin filaments suggesting a different nucleating mechanism (Michelot *et al.*, 2006). Nucleating and actin bundling activity of AtFH1 depends upon FH1 domain, however FH1 alone cannot bind actin (Michelot, 2005). It seems that FH1 modulates FH2 pointy end capping function to a loose capper which accelerates elongation (Michelot, 2005).

fh1 LOF mutants exhibit cotyledon epinasty and more importantly, larger and less circular pavement cells as a result of defective lobbing (Rosero *et al.*, 2016). The development of jigsaw puzzle-like pattern of cotyledon pavement cells is a process tightly mediated by both actin and microtubule cytoskeleton network. Lobes are shared between neighbouring cells and thus shaped from two sides. The concave side of the lobe forms trough tip growth maintained by actin filaments. Meanwhile microtubules define the site of growth by directing microfibrils which are deposited perpendicular to the lobe margin at its convex side (Armour *et al.*, 2015). Fluorescently labelled microtubules accumulated at the cortex in the neck region of lobes and showed decreased lateral movement in *fh1* pavement cells. *fh1* and wt plants respond differently to cytoskeletal drugs. Taxol treated root elongation was less affected in *fh1* seedlings indicating a possible resistance to microtubule inhibitors. Similar results have been observed in oryzalin treated plants. Cotyledon pavement cells treated with oryzalin had less pronounced lobes in wt plants in contrast to *fh1* which showed no change in circularity. However *fh1* had enlarged cells after treatment, which could not be explained by simple resistance. Enlargement could be abolished with LatB, thus cell expansion seems to be mediated rather by actin than MTs. It has been observed in rhizodermis cells that actin network treated with FH2 inhibitor SMIFH2 mimics the effect of FH1 mutation (Rosero *et al.*, 2013; Rosero *et al.*, 2016).

Class II formins

FH13

FH13 is a typical Class II formin that contains PTEN domain and could potentially link actin to membranes. So far, no published report on this gene exists; from large scale

transcriptomic studies it is known that is expressed mostly in pollen and seeds (http://bar.utoronto.ca/efp2/Arabidopsis/Arabidopsis_eFPBrowser2.html). Phenotype of loss of function mutations is subtle, if any. It has been suggested that FH13 inhibits lateral root formation. Based on observation from few experiments revealing that *fh13* has more lateral roots and thus FH13 gene might be responsible for inhibition of branching in seedlings, it has been suggested, that this phenotype could be enhanced by drought (Přerostová, 2011).

FH14

FH14 (or AFH14) is also a typical Class II formin containing a PTEN-like domain. It promotes nucleation of actin filaments but also acts as a negative regulator of actin filament elongation (Zhang *et al.*, 2016). FH14 binds to actin filament barbed-end in form of a dimer inhibiting elongation by 90% compared to actin alone. Affinity was found high compared to other plant formins. Observations were done *in vitro* with fluorescently labelled SNAP-549-FH14. Fh14 competes with capping protein ABP29 at barbed ends. Fh14 combined with various plant profilin isoforms promotes elongation rate 10 to 42 times (Zhang *et al.*, 2016).

FH14 has also been tested for interaction with both actin filaments and microtubules (Li *et al.*, 2010). Results show that FH14 FH1FH2 binds both MTs and actin filaments *in vitro*. Furthermore, FH14 FH1FH2 was able to bind free actin and promote nucleation. In fact, FH2 domain alone could bind both cytoskeletal polymers.
Bundling was also reported in both cases. More interestingly, when preformed microtubules were added into solution with AFs bundled with FH14 FH1FH2, actin bundles began to dissolve and MTs started bundling. It has been suggested that FH14 FH1FH2 detached from AFs for its affinity is stronger to MTs. This has been confirmed by performing the experiment in a reverse order. Microtubules remained bundled while microfilaments remained scattered randomly, concluding that microfilaments could not strip FH14 FH1FH2 off MTs. FH14 FH1FH2 added into solution with both cytoskeletal polymers promotes microtubule bundling preferentially.

Fluorescent visualization revealed colocalization of FH14 with microtubules in spindle and phragmoplast of dividing cells. Oryzalin treatment (10 μM, 15min) confirmed these observations. Along with disruption of microtubule structures FH14 dissolved. Overexpression of FH14 supressed the effect of oryzalin by 23%. Similar results were

achieved with actin cytoskeleton. FH14 colocalized with microfilaments in dividing cells. Overexpression supressed the effect of LatB (200 n, 50 min) by 33,8%. These results indicate that FH14 binds to both AFs and MTs with a higher affinity to MTs (Li *et al.*, 2010).

Plants with decreased FH14 expression (by estrogen-induced microRNA construct) show spectrum of changes in mitotic apparatus. LOF plants have incorrectly divided microspores in 40% of cases. Alterations were observed in particular phases of microspore generation showing skewed radial microtubular system in telophase, irregular orientation of mitotic spindle and distribution of nuclei leading to 2n dyad, triads and polyads also lacking the “swollen region”, a typical feature of a wt tetrad (Li *et al.*, 2010)

So far, it seems that FH14 FH2 is responsible for binding and bundling both AFs and MTs. However, FH2 domain might contain sequences with overlapping functions able to bind only one or the other. Consistent with this hypothesis, cytoskeletal polymers seem to compete with each other. On the other hand, excess of FH14 FH1FH2 could promote MT bundling with AF. Crosslinking has been observed in Drosophila formin Cappuccino (Rosales-Nieves *et al.*, 2006). It has been suggested that the conserved FH1FH2 domain acts as a dimer or tethered dimer (Kovar, 2006; Michelot *et al.*, 2006). Though multimers of different sizes were observed in mouse mDia1 (Li and Higgs, 2003), it is unclear whether the behaviour of FH14 is of a similar nature.

Physiological function of FH14 is yet to be revealed. So far it seems that FH14 has a role different from cortical cytoskeletal linkers, since it decorates mitotic structures but has not been observed in the cortex such as the moss FH14 (Vidali *et al.*, 2009).

Objectives

The main objective of this study is phenotypic characterization of early root system development in *Arabidopsis* FH13, FH14 and double FH13 FH14 LOF mutants. The two genes encoding class II formins, FH13 (At At5G58160) and FH14 (At At1G31810) were chosen since they are two closely related and typical representatives of their clade in *Arabidopsis*. Though FH14 has been explored previously (Li *et al.*, 2010)(see introduction, FH14), the function of FH13 is yet unknown. Phenotypes of loss of function mutants are not immediately obvious due to functional redundancy. It is also possible that FH13 and FH14 might act as a dimer (Houšková, 2015).

Secondary methodological aim derives from the necessity to establish a reliable and reproducible method for root system imaging and evaluation.

Based on previous observations documenting that mutations in the Class I formin FH1 affect pavement cell shape (Rosero *et al.*, 2013) and that mutations impairing the other actin-nucleating system in plant cells, the Arp2/3 complex affect epidermal permeability (Deeks and Hussey, 2003), we also investigated whether these characteristics are altered in *fh13, fh14* and double *fh13xfh14* mutants.

The experiments have been performed on developing roots, since root elongation is a result of intensive anisotropic growth regulated by both actin filaments and cortical microtubules. If FH13 and FH14 are involved in F-actin microtubule crosstalk we should be able to observe alterations in root growth. I expect that cytoskeletal drugs will enhance mutant phenotype, as previously shown for class I formin FH1.

Methods

Biological materials

All plants were obtained from seed collection at the department of experimental biology, laboratory of cell morphogenesis and previously used in work by Lenka Stillerová (Stillerová, 2014) *FH13* and *fh14*, *fh13*xwt(+/+) and *fh1(Rosero* et al*., 2016)*. Plants were grown on jiff pellets ex vitro growth chamber, 16h light 8h dark period, irradiation 100µmol/m^2/s. In vitro cultivation conditions are described in detail in a separate section of Methods below.

Plant genotypes and genotyping

Arabidopsis thaliana T-DNA insertional mutants were originally provided by SALK, three for each gene: *FH13* (*fh13*-1, SALK_064291C, *fh13*-2, SALK_035314; *fh13*-4, SALK_071310) and *fh14* (fh14-1, SALK 058886; *fh14*-2, SALK 038277; *fh14*-3, SALK 021011) (Figure 2, Figure 3). The presence of wt or mutant alleles was determined using PCR (see Polymerase chain reaction (PCR)) and primers (described in Table 1).

Mutant alleles were determined using the combination of RP primers with SALK primer LBb1.3 (ATTTTGCCGATTTCGGAAC) (signal.salk.edu/tdnaprimers.2.html).
Predictions for product length were obtained from public website. Mutants were crossed in order to create *fh13* and *fh14* double mutants. Control lines containing two Wt(+/+) alelles have been selected from *fh13*-1 and *fh14*-1 heterozygotes originally obtained from SALK and used as controls. For comparison, *fh1* has been also included in the experiment (*fh1*-1, SALK032981.52.75 (Rosero *et al.*, 2013)).

description	clone	LP	RP
fh13-1	SALK_064291C	TTTGACCTAATGGTGGTGGAG	GTTTCAGCAGTTAGCCATTGC
fh13-2	SALK_035314	GTGTGTTGCAGTGTTCGATTG	ACCACTCGAAACATCATGACC
fh13-4	SALK_071310	AACCAAGTTATCCCCATCTGG	TTGTACCAGTTCGCATTTTCC
fh14-1	SALK_058886	ACCACTCGAAACATCATGACC	ATTCTGCCTGGAGCCATATG
fh14-2	SALK_038277	AATCGCAATGCTTATTCGAAG	CTCGATGTCCTTTTGAGCAAG
fh14-3	SALK_021011	TCTGTACCATATGGCTCCAGG	GAAACTAGGGAGAGGTGGTGG

Table 1. Overview of SALK lines and primers used for genotyping obtained from (signal.salk.edu/tdnaprimers.2.html).

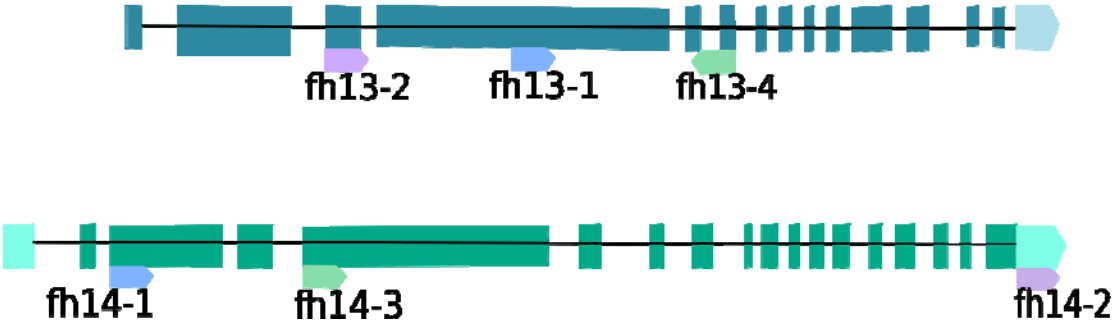

Figure 2. Schematic picture showing exon sequence of *fh13* and *fh14* genes with marked insertions provided by SALK (signal.salk.edu/tdnaprimers.2.html): fh13-1 insertion is placed in the fourth exon, fh13-2 in second exon, fh13-4 after fourth exon; fh14-1 in the second exon, fh14-2 on th 3'UTR, fh14-3 in the fourth exon of the gene.

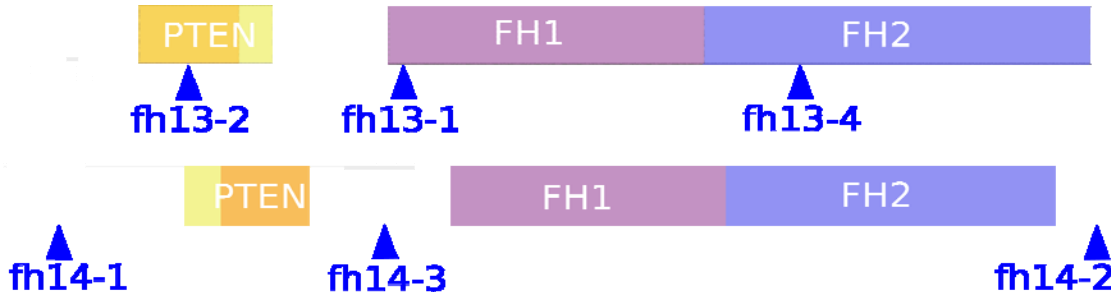

Figure 3. Schematic picture showing predicted protein sequence of AtFH13 and AtFH14 with marked insertions and domains (www.arabidopsis.org)

DNA isolation

(Stillerová, 2014)

Young *Arabidopsis* leaves approximately 1cm in diameter were harvested, crushed, homogenized in a 1,5ml Eppendorf tube with a plastic stick in 200µl extraction buffer (200mM Tris-HCl pH 7,5, 250mM NaCl, 25 mM EDTA, 0,5% SDS). 300µl of chloroform was added to the sample and vortexed for 5 minutes, then centrifuged for 3 minutes at 13000 rpm speed. 150ml of supernatant was transferred into a fresh tube and 150ml isopropanol added to the sample. After a short mix the sample was kept in freezer -20°C for 10 minutes. When DNA precipitated, it was centrifuged again at 13000 rpm peed for 5minutes. Supernatant was discarted and remaining DNA was dried on the bottom of the Eppendorf tube. After approximately one hour the DNA was diluted in 40 µl of distilled water and stored in 4°C.

Polymerase chain reaction (PCR)

PCR was preformed using DreamTaqTM polymerase. One reaction contained 16,31µl distilled water, 2µl DreamTaqTM reaction buffer, 0,25µl dNTP(10mM), 0,2 µl primer R and 0,2 µl primer L, 0,04 µl DreamTaqTM polymerase and 1µl of the isolated DNA. Samples were kept on ice in 200ml PCR tubes. The PCR program was set for 94°C 2:00 min., 94°C 0:30 min, 59°C 1:00 min., 72°C 1:45 min., 72°C 10:00 min., 2nd-4th step was repeated 30x using cycler TPersonal from Biometra or gradient cycler TGradient, Biometra. Product was kept on ice adding 4µl of Loading die to each sample for visualization with electrophoresis. 10ml of the product was transferred into each hole in gel containing 1% agarose diluted in 1xTBE (Tris, boric aacid, EDTA) and 0,001% GelRedTM. GeneRulerTM DNA Ladder Mix (0,5µg/µl) was used as reference. Electrophoresis was done at 70V. The gel was then visualized in G:BOX, Syngene and photographed with program GeneSnap, Syngene.

Crossing

Homozygous mutant plants *fh13* were crossed with *fh14* under binocular magnifier. Flowering adult plant, which was to serve as mother, was deprived of most of the flower buds leaving only 3 to 4 non-opened. The buds were stripped leaving just gyneceum and the pistil. Pollen from post-anthesis stamens from the father plant was carefully spread onto the pistil. The flower was wrapped in plastic foil. Mother plants

were kept in growth chamber until seeds maturated. F1 generation was reproduced and F2 generation genotyped in order to select homozygous lines lacking both functional FH13 and FH14.

In vitro culture and inhibitor treatment

Arabidopsis seeds were kept in -20°C for 48 hours after harvest to prevent insect contamination. Sterilized in 70% EtOH for 1 minute and 10% SAVO for 10 minutes, then washed with distilled water five times in flow-box. Sterilized seeds were spread on Petri dishes with MS (Murashige Skoog, 1962) medium containing 1% agarose, 1% sacharose. Stratification took 2 days at 4°C in darkroom followed by germination 4 days, 22°C with 16h light and 8h dark period and irriadiation 100µmol/m^2/s. After 4 days, germinated plants were transferred to media containing low doses of cytoskeletal drugs (as described below) and scanned using the MULTISCAN/BRAT phenotyping platform every 24h for 3 days.

Inhibitor treatment followed protocol described in paper by Amparo Rosero (Rosero *et al.*, 2013). Seeds were placed on square plates containing MS medium (containing 1% agarose, 1% sacharose) with treatment in two rows for germination. Since growth is enhanced in the lower part of the plate, seedlings of each genotype were distributed evenly between the top and bottom rows in order to eliminate potential differences. Workflow is described in Figure 4a.

Oryzalin and latrunculin stock solutions stored in -20°C were diluted in dimethylsulfoxyde (DMSO) and added to liquid agar media in concentrations at 0,01mM oryzalin and 0,005mM latrunculin. The control media contained DMSO 0,1%(v/v). DMSO, latrunculin and oryzalin were purchased from Sigma.

A

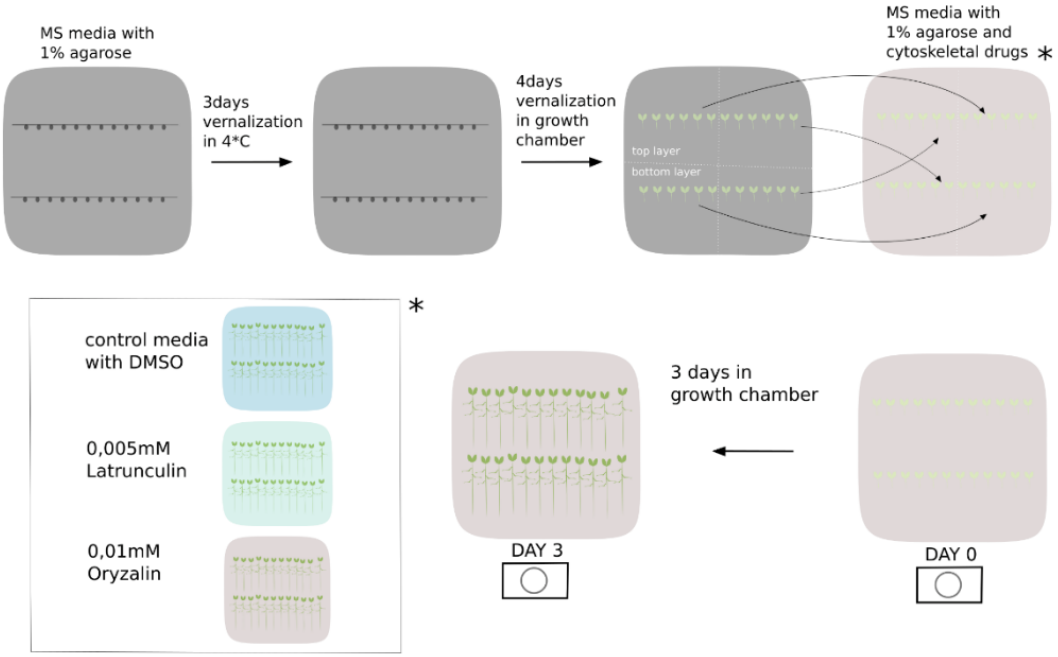

B

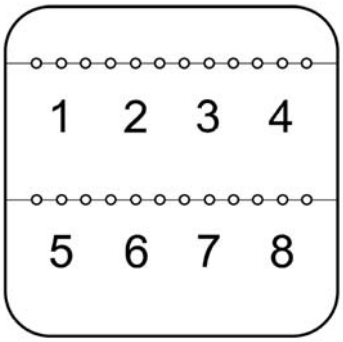

Figure 4. Schematic picture of experiment design showing distribution of seedlings on plates. Asterisk refers to two types of media containing cytoskeletal drugs and control media (see Concentration optimization) (A). Grid layout template provided by BRAT manual (B).

Root scanning and image analysis

MULTISCAN

Images of the plates were taken with Multi-CCD Flatbed Scanner Cluster with the resolution 1200 dpi, which is theoretically equivalent to a resolution of 21 mm/pixel, controlled by the MULTISCAN software (Slovak et al., 2014) Scanners were designed for scanning square plates. Seedlings had to be placed in exact positions using grid layout template (Figure 4b).

BRAT

For subsequent analysis of acquired images, BRAT (Busch Lab Analysis Toolchain), a software package designed to quantify root triats of *Arabidopsis taliana* seedlings (Slovak *et al.*, 2014), has been used. BRAT has been integrated as a FiJi plug-in (Schindelin *et al.*, 2012). BRAT works as an automated pipeline for images in a specified directory. It can align the images and track time series on several different treatments. Seedlings are identified and analysed. After images are processed the user is allowed to do a supervised quality control and reject incorrectly segmented roots or check the erroneously identified roots manually. Once the quality control is done, the data is processed and results are generated in the form of text files. For every experiment three files are generated. One contains trait values for each plant in every time sequence, second provides values over time and third statistical summary. BRAT can measure root length, width, growth rate and growth direction. For comparison, length has been also measured manually in imageJ version 1.51w.

Quantitative evaluation of pavement cell shape

Arabidopsis seeds were vernalized for 2 days in 4°C dark, then cultivated on MS, 1% sucrose, 1% agarose in 16h light, 8h light period, irridation 100μmol/m^2/s for 10 days.

Images were taken from cotyledons in the area between midrib and the edge of each cotyledon.

Confocal microscopy has been done with Leica TCS SP2 (lens 25x). Images were manipulated in imageJ for better visualization of cell borders. Individual steps were done for each stack of images in Z-projection as follows: Process -> smooth, Process -> Binary -> make binary, Process -> binary -> skeletonize. Since some parts of the

image were out of focus and the skeletonized picture did not recognize cell walls as a full line they had to be filled in manually with paintbrush tool (Figure26). Only than area, perimeter and circularity could be measured.

Evaporation test

Leaves were taken from adult plants with a full-grown rosette but not yet elongated generative shoots. Plants were grown for 28 days. Two leaves 5th and 6th have been taken from each plant and weighed immediately. Leaves were kept on blotter sheet in room temperature and weighed with 30 minute frequency six times and then once more after an hour.

Data handling and statistical tools

Obtained data had to be handled with appropriate statistical process. For experiments with two types of drug treatment statistics has been calculated with 2way ANOVA (https://www.wessa.net/rwasp_Two%20Factor%20ANOVA.wasp). 1way ANOVA (http://astatsa.com/OneWay_Anova_with_TukeyHSD/) has been used comparing genotypes in conditions where only one factor (genotype) was studied, such as pavement cell circularity and evaporation test. For categorical data obtained from root count we used Chi square (http://www.quantpsy.org/chisq/chisq.htm), which provided *p*-value when comparing mutant to wtor Yates' *p*-value if t least 20% of expected frequencies were less than 5. Obtained *p*-values have been corrected for false discovery rates with Benjamini-Hochberg procedure (https://www.sdmproject.com/utilities/?show=FDR).

Each experiment was repeated several times P-values <0,05 which were reproducible in several independent experiment are considered as relevant.

Results

Establishing a reliable method for root growth evaluation

Image analysis

There have been a few problems while processing images. BRAT often failed to recognize objects as seedlings and align it in a time series. Also the user has to be

careful when naming each image in a time series giving it the same `plate identifier' number found in the BRAT manual (Slovak *et al.*, 2014) otherwise the software cannot align it. However, there might be more problems such as incorrect identification of the hypocotyl (Figure 5, Figure 7) non-identifying much of the seedlings (Figure 6) or even an entire plate. This has caused loss of data up to 25% (Figure 8). Measuring roots manually using ImageJ turned out to be a more reliable method. Values displayed in this work were obtained by measuring roots manually in order to keep consistency in results.

A

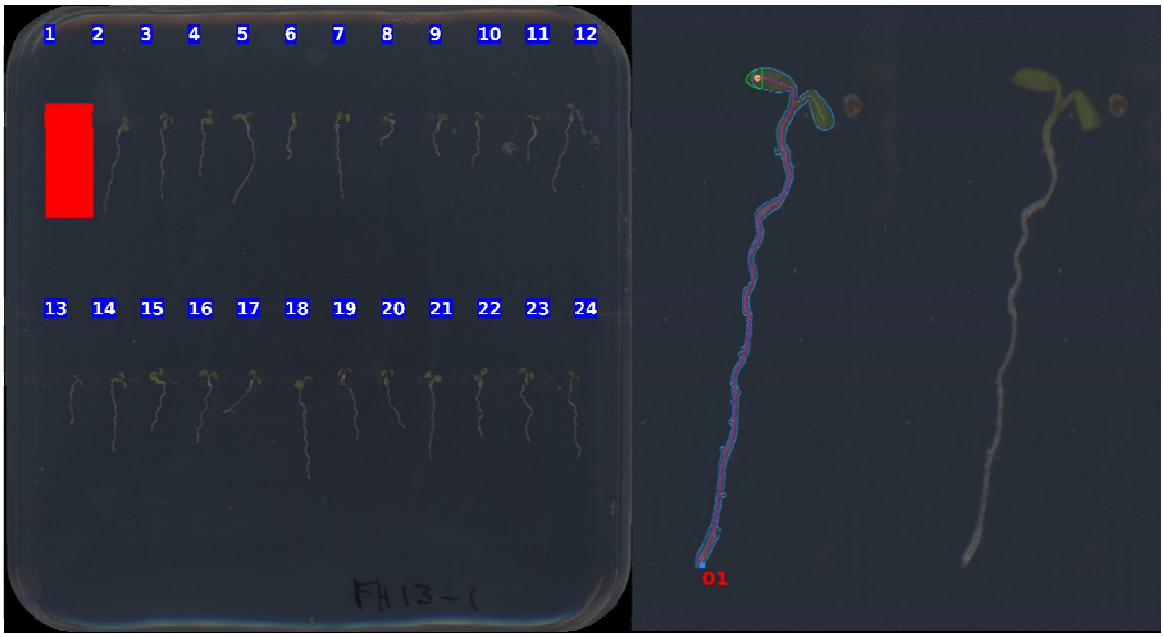

B

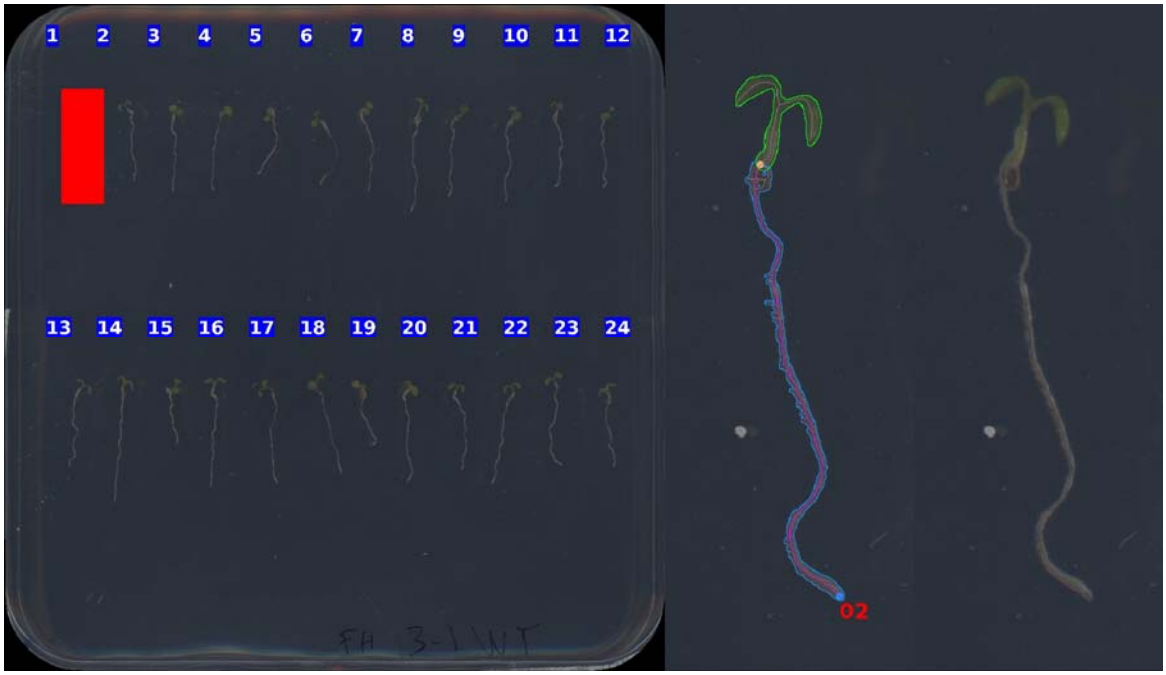

Figure 5. Scan of 7DAG seedlings with identified hypocotyl and root by BRAT incorrectly (A) and correctly (B).

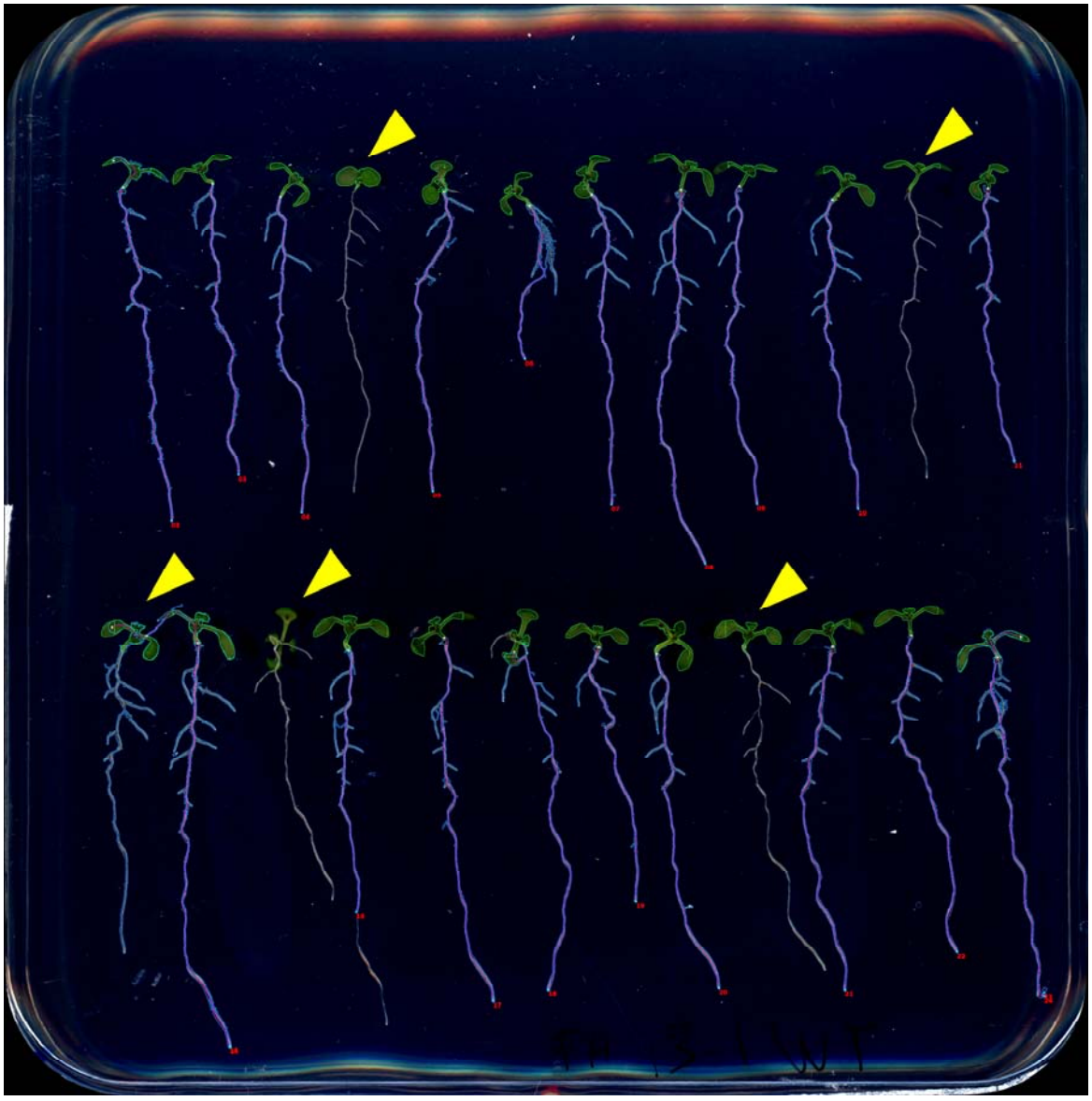

Figure 6. Scan shows overall view of an entire plate with incorrectly identified roots marked with yellow arrows (C) Images have been adjusted in imageJ.

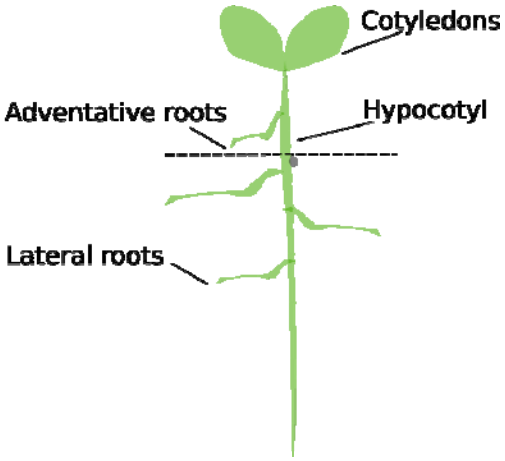

Figure 7. Drawing of Arabidopsis seedling explaining position of hypocotyl, adventitious and lateral roots.

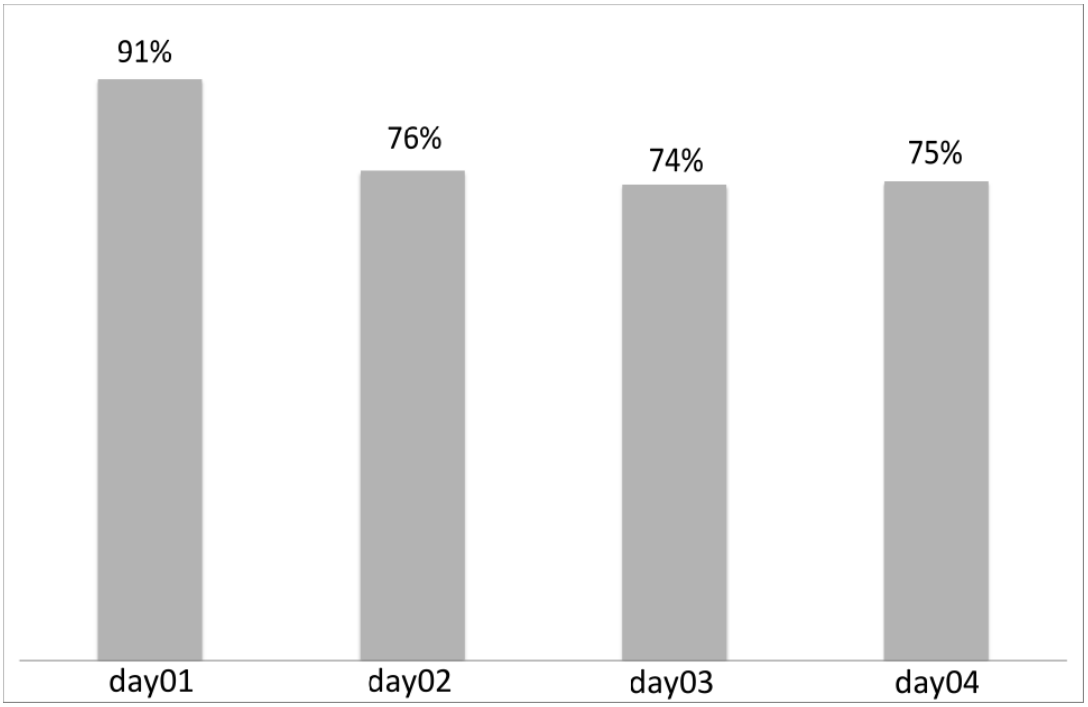

Figure 8. Efficiency of BRAT software in % of correctly evaluated roots in a time series Data from oryzalin (0,01mM) treated seedlings.

Experimental design

FH13 and FH14 phenotypes seem to be very subtle and uneasy to detect. In order to enhance hypothetical defect in growth, we applied various cytoskeletal drugs on developing seedlings. Since formin seems to affect both microtubules and actin filaments two types of treatment have been used (Figure 4a): oryzalin, which inhibits microtubule assembly and latrunculin, which inhibits actin filament growth. A reliable method has been established testing three SALK lines for each gene FH13, FH14 and their relative wt in two different treatments and control conditions. I measured root length, number of adventitious and lateral roots, weight loss during desiccation and epidermal cell shape. From collected data it is obvious that wt has been significantly inhibited by the treatment assuming that cytoskeletal drugs have proved their biological activity. Mutant lines have been compared with wt, in order to reveal alterations such as hypersensitivity, resistance or whereas mutation mimics the effect of treatment. Phenotypes have been evaluated and analysed with relevant statistical tools. Results presented in this study have been collected from four independent experiments.
I have also successfully crossed *fh13* and *fh14*. Obtained double mutants were also included in our experiments.

Controls and wild types

At the beginning we considered as necessary to keep specific control lines for each formin mutant. Wt has been obtained from previous studies (Stillerová, 2014). Homozygous *fh13*-1xWT++ (SALK_064291) and *fh14*-1xWT++ (SALK_058886) have been obtained by back-crossing heterozygous *fh13* and *fh14* (Figure 9, Figure 11).

Though homozygosity of used plants has been tested by genotyping, *fh14*-1xWT++ showed variability within the population. Furthermore, drug treatment experiments revealed significant phenotype of *fh14*-1WT++ compared to Col-8 (Figure18). Thus, we suspect an additional insertion in *fh14*-1 line. Unfortunately, it is unclear what specifically causes this phenotype. I thus consider phenotype in *fh14*-1 mutants interesting but difficult to interpret.

Columbia 8 has been also included in the experiments. Wild types have been compared with each other in multiple conditions with two way ANOVA in an

independent experiment. No significant differences have been detected and thus all ware considered as commutable. In order to simplify the results *fh13*-1xWT++ has been chosen as a relevant control for all seven SALK lines presented.

Fh1-1 has been included in the experiment as another control. It has been found in previous studies that *fh1-1* LOF mutants are resistant to low doses of oryzalin. This control is necessary in order to check the biological activity of the chemicals and to set correct concentration of oryzalin.

A

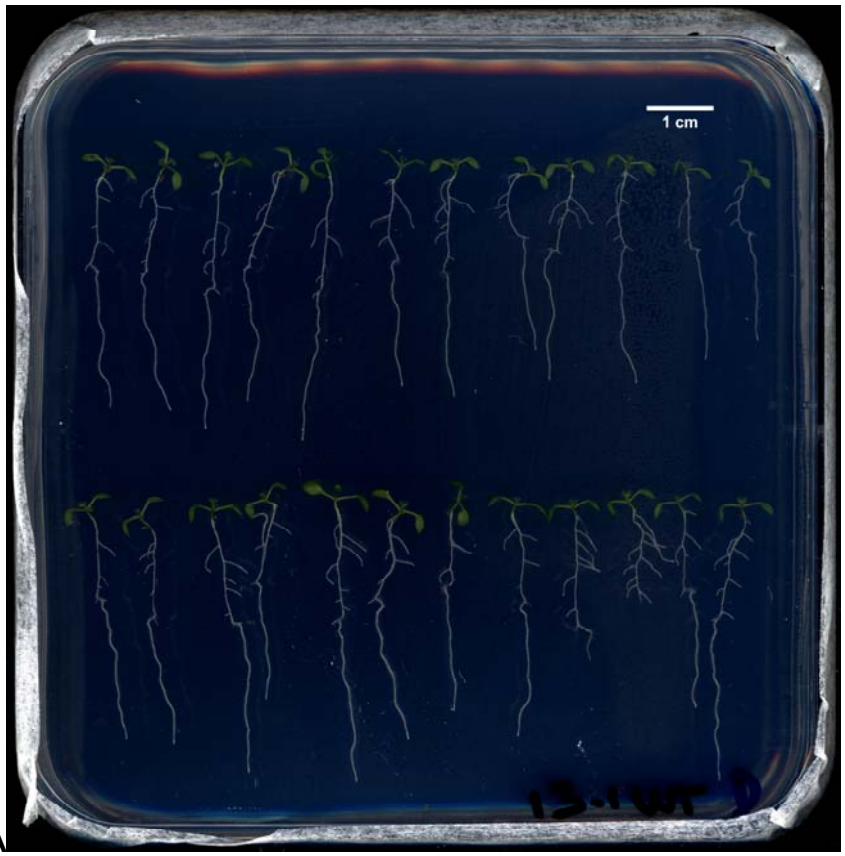

B

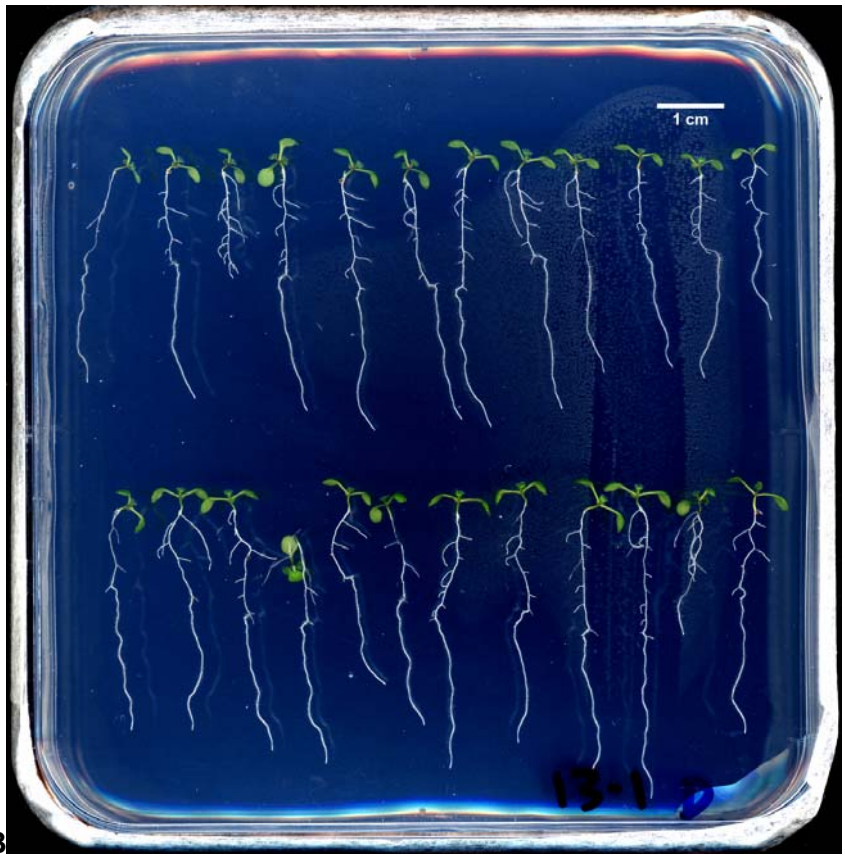

C

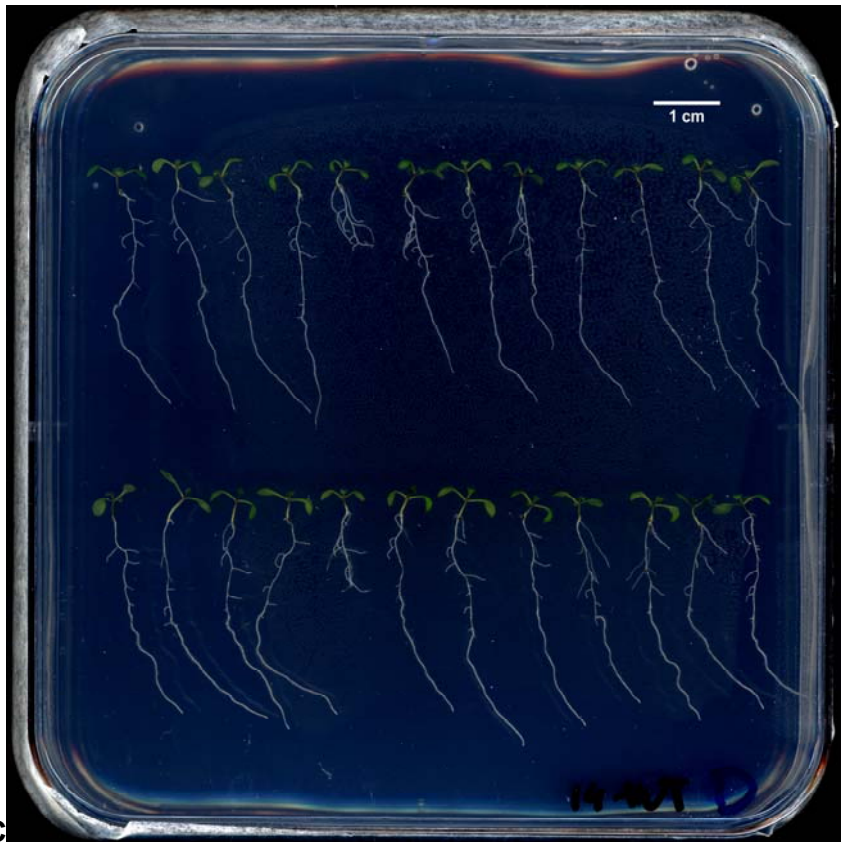

D

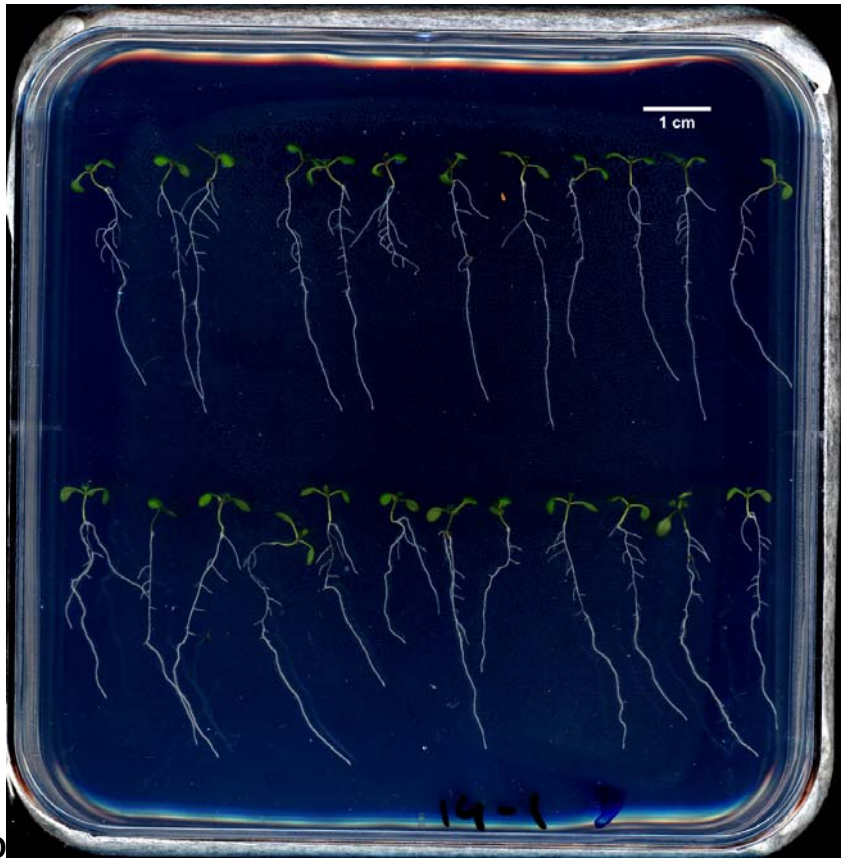

E

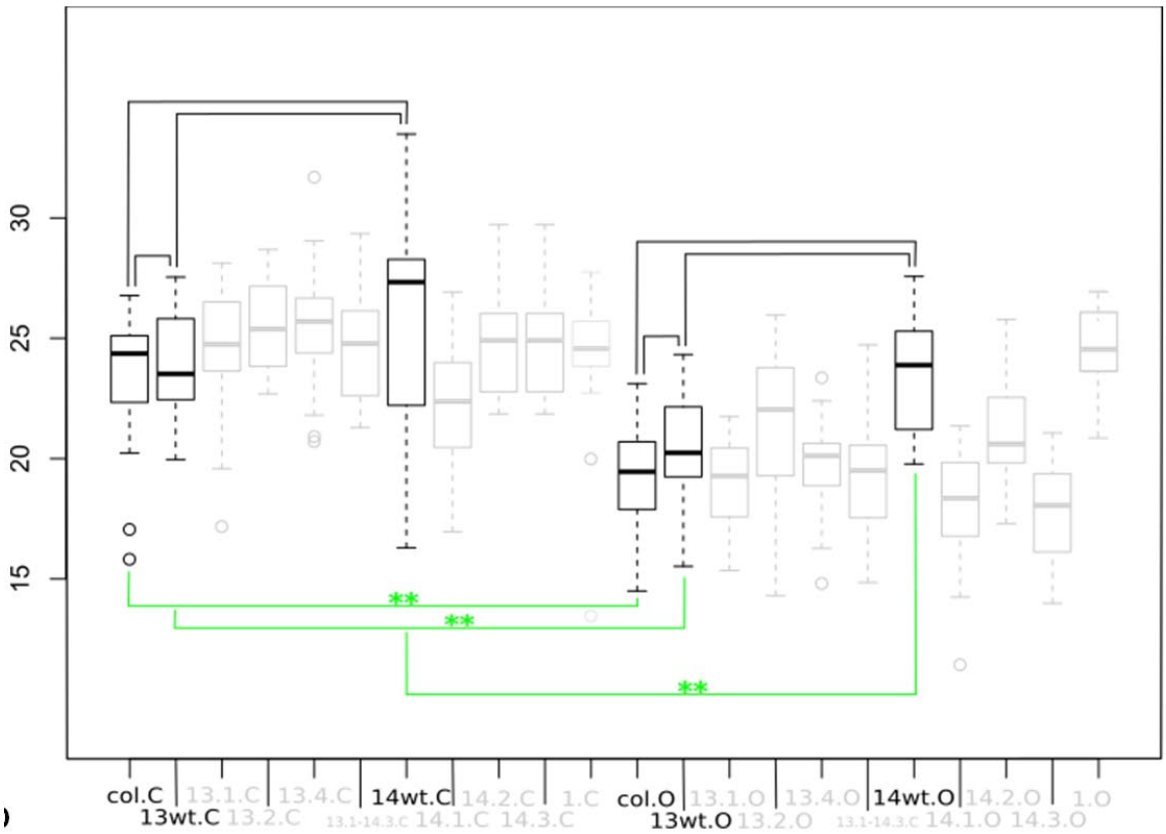

Figure 9. Representative scan of fh13-1xWT++(A), fh13-1(B), fh14-1xWT++(C), fh14-1 (D) lines, 7 DAG seedlings on control media. Image has been adjusted in imageJ. Boxplot graph showing significant differences between three types of WT. Data has been obtained by measuring root length of 7DAG seedlings after 3 days on control media and on 0,01mM oryzalin (E)

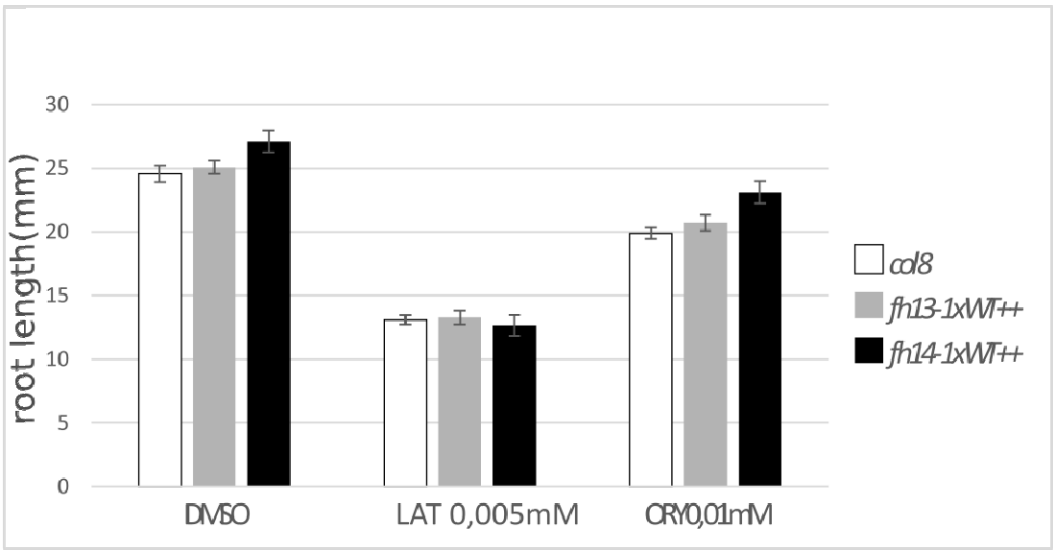

Figure 10. Graph showing root length differences between wild type seedlings, 7DAG old after 3 days on 0,01mM oryzalin and 0,005mM latrunculin treatment and Control media. Asterisk highlights significant differences between treated and non-treated plants **p<0,01;*p<0,05

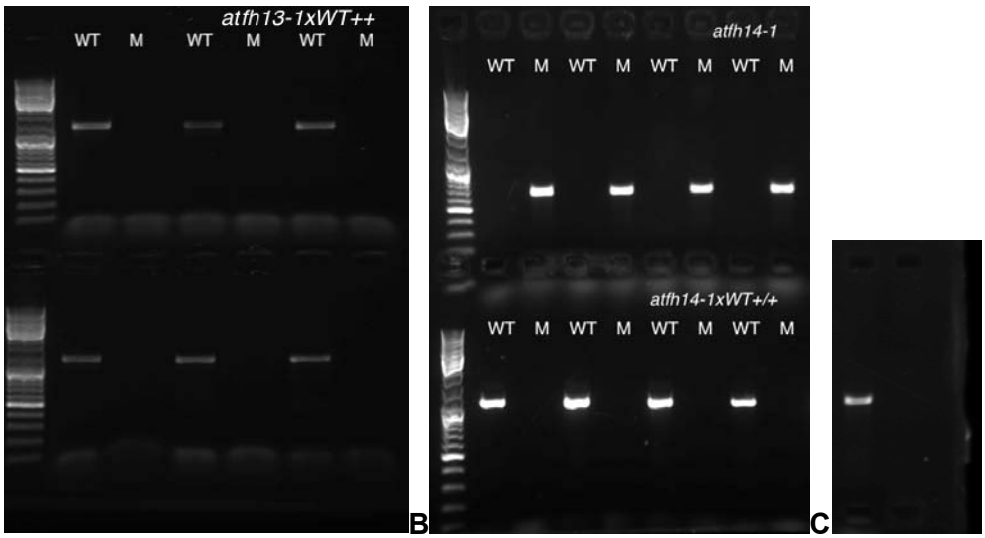

A **B** **C**

Figure 11. Results from genotyping visualised on agarose gel shows bands in the area of shorter PCR product for mutant and longer for WT. Homozygous fh13xWT+/+ (A), homozygous fh14-1 -/- and fh14-1xWT+/+ (B), Col-8 (C)

Concentration optimization

Based on previous studies oryzalin concentration has been set at 0,01mM. latrunculin seems to have a stronger effect on growth and had to be reduced to half dose 0,005mM. Lower doses had an insignificant effect on wt and higher doses supressed growth to a point where potential differences between genotypes could no longer be detected (Figure 12).

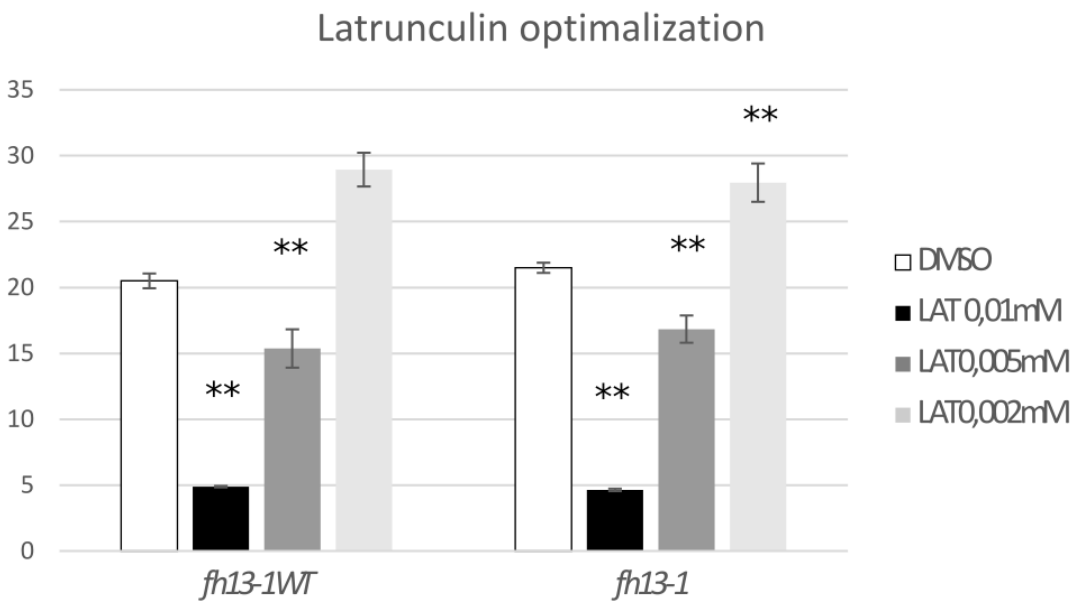

Figure 12. Graph showing increment in root length of 7DAG seedlings after 3 days on latrunculin treatment of variable concentrations and Control media without treatment. Asterisk highlights differences between genotype and a relevant wtp<0,01;*p<0,05**

Root growth in time series

Root growth has been monitored every 24 hours for three days. There has been a gradual inhibition after placing *fh13* seedlings on media with oryzalin treatment (Figure 13). Growth was monotonous and thus we decided to evaluate the final length after three days on treatment and compared it with initial length.

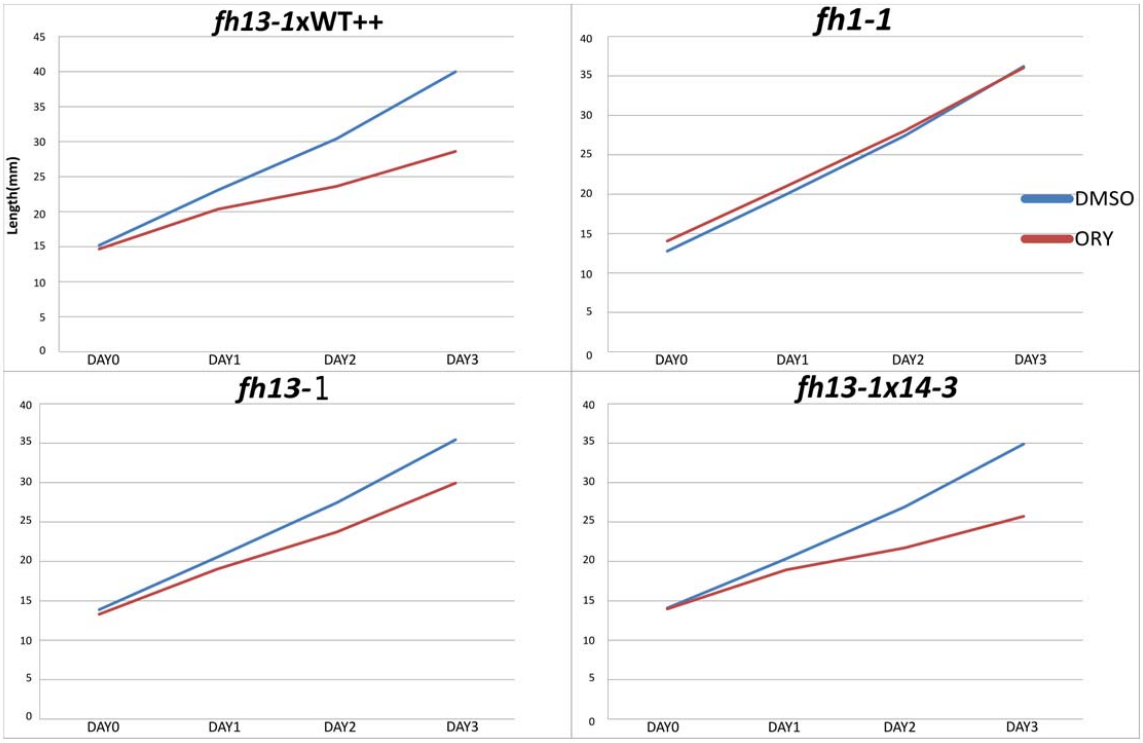

Figure 13. Growth of 4 DAG seedlings after replacement onto 0,01mM oryzalin treated media in time series from day0 to day3.

Effect of drug treatment on formin mutants

Main root length

Two-way ANOVA is able to compare all genotypes with each other. The following boxplots with marked p-values show statistically relevant differences between mutant lines (Figure14 and Figure18). For better orientation in our results, we have formulated three questions: Q1 Does mutation effect root growth? Mutant lines have been compared with relevant wtto reveal potential influence of mutation (on latrunculin Figure 15 and and Oryzlin Figure 19) Q2: did the treatment effect growth? This can be

answered by comparing treated and non-treated plants (on latrunculin Figure16 and oryzalin Figure20). Q3: Do mutant lines differ from each other? (on latrunculin Figure17 and and oryzalin Figure21).

Consistent with previous studies *fh1* shows resistance to oryzalin (Figure19). No other similar resistance has been detected in the rest of mutant lines. *fh14*-2 has significantly longer roots than *fh14*-1 on oryzalin treatment (Figure21). Latrunculin treatment did not reveal phenotype of any significance in terms of root length (Figure15 and Figure17).

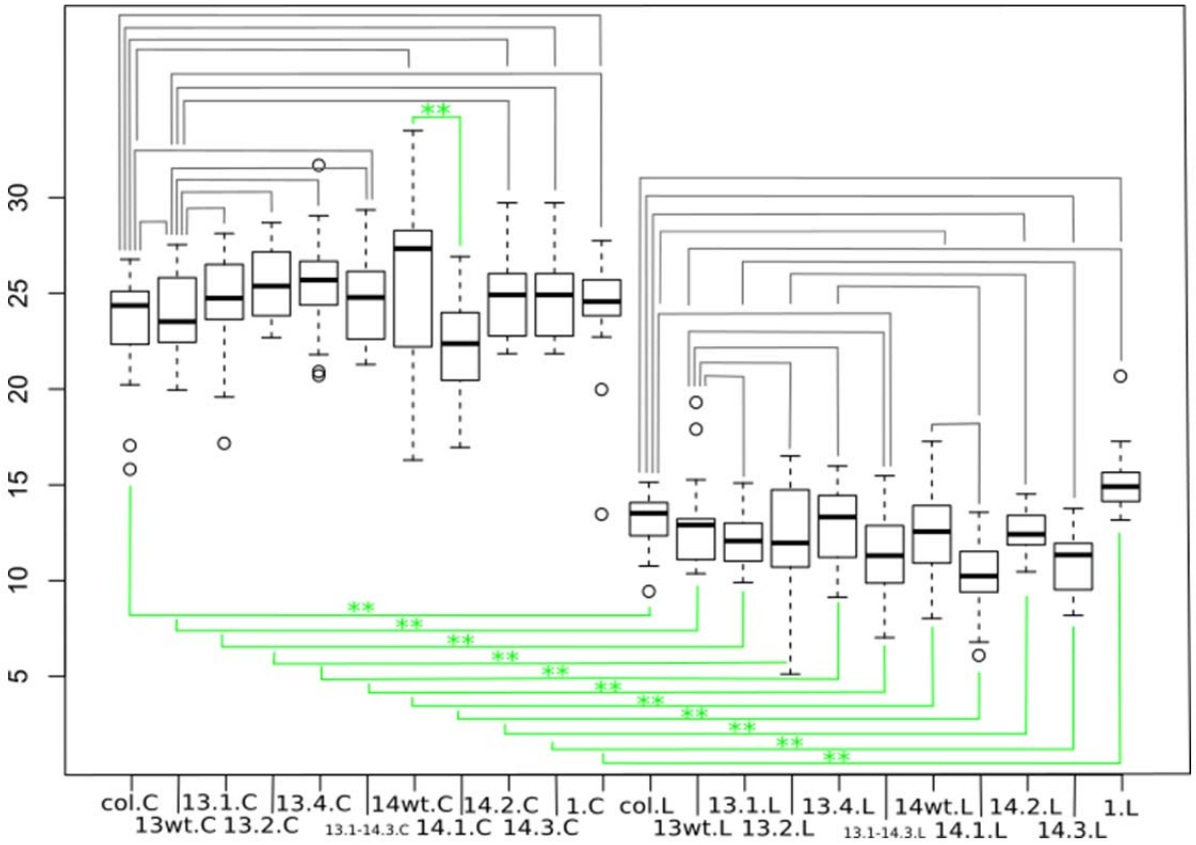

Figure 14. (Q1 top half + Q2 bottom half) boxplot graph showing root length of 7DAG seedlings after 3 days on 0,005mM latrunculin treatment (L) and Control media without treatment(C). The relevant combinations of compared genotypes have been marked with a clamp and highlighted with asterisk in case of significance, genotypes compared with wt(upper half of the graph), treated and non-treated plants (lower part). **p<0,01;*p<0,05.

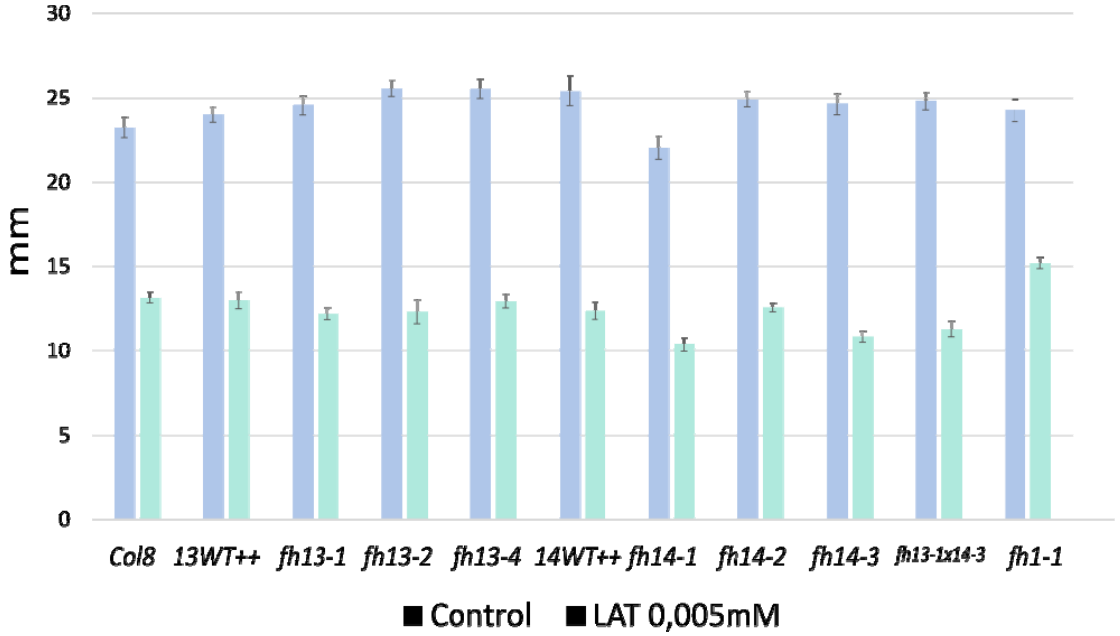

Figure 15. (Q1) Graph showing average root length of 7DAG seedlings after 3 days on 0,005mM latrunculin treatment (L) and Control media without treatment(C). Asterisk highlights differences between genotype and a relevant wtp<0,01;*p<0,05**

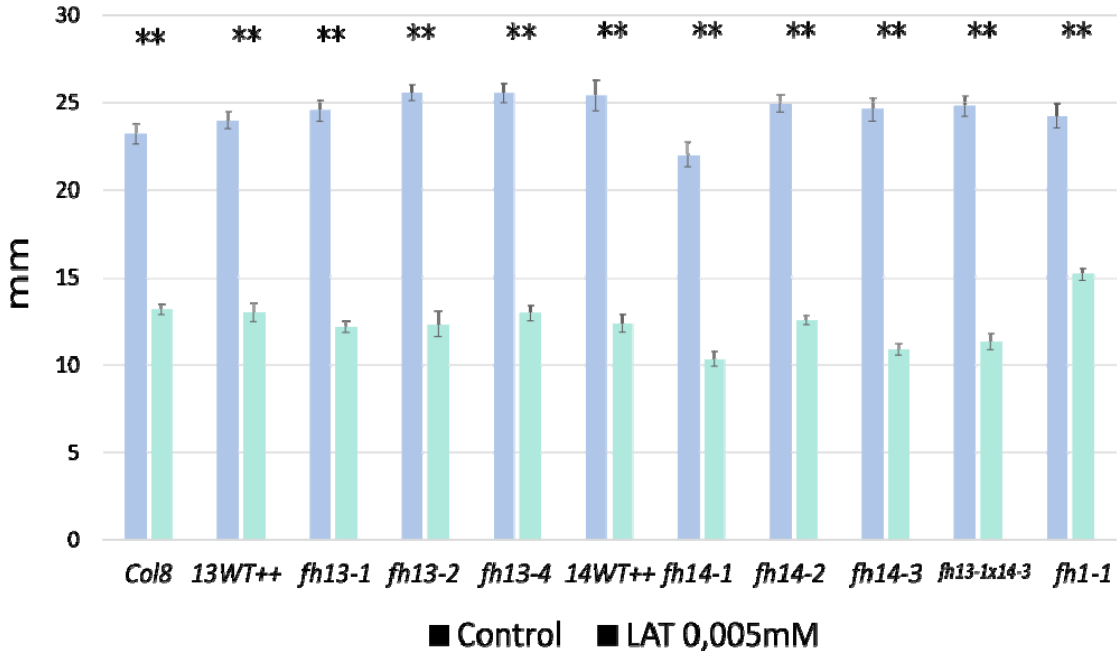

Figure 16. (Q2) Graph showing average root length of 7DAG seedlings after 3 days on 0,005mM latrunculin treatment (L) and Control media without treatment(C). Asterisk highlights significant differences between treated and non-treated plants **p<0,01;*p<0,05

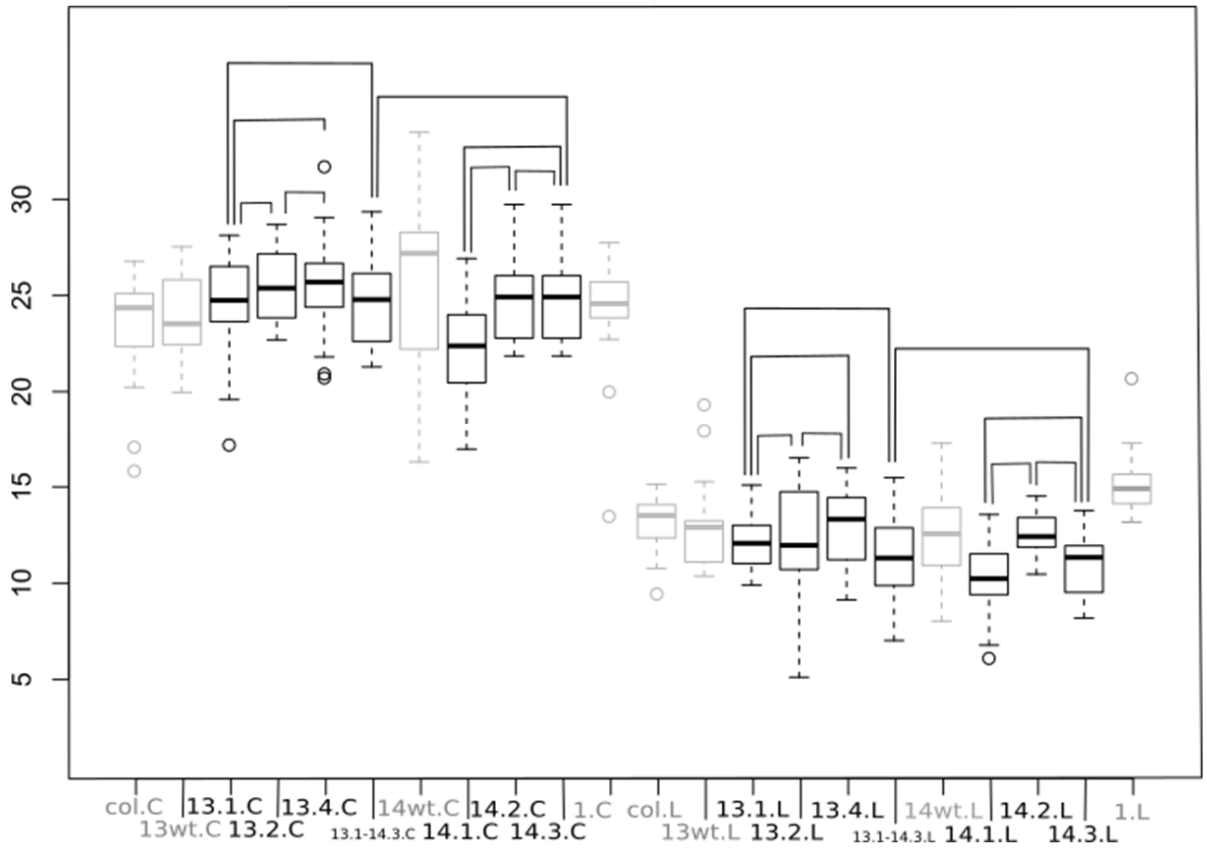

Figure 17. (Q3) boxplot graph showing root length of 7DAG seedlings after 3 days on 0,005mM latrunculin treatment (L) and Control media without treatment (C). Genotypes compared with each other have been marked with a clamp and highlighted with asterisk in case of significance. **p<0,01;*p<0,05

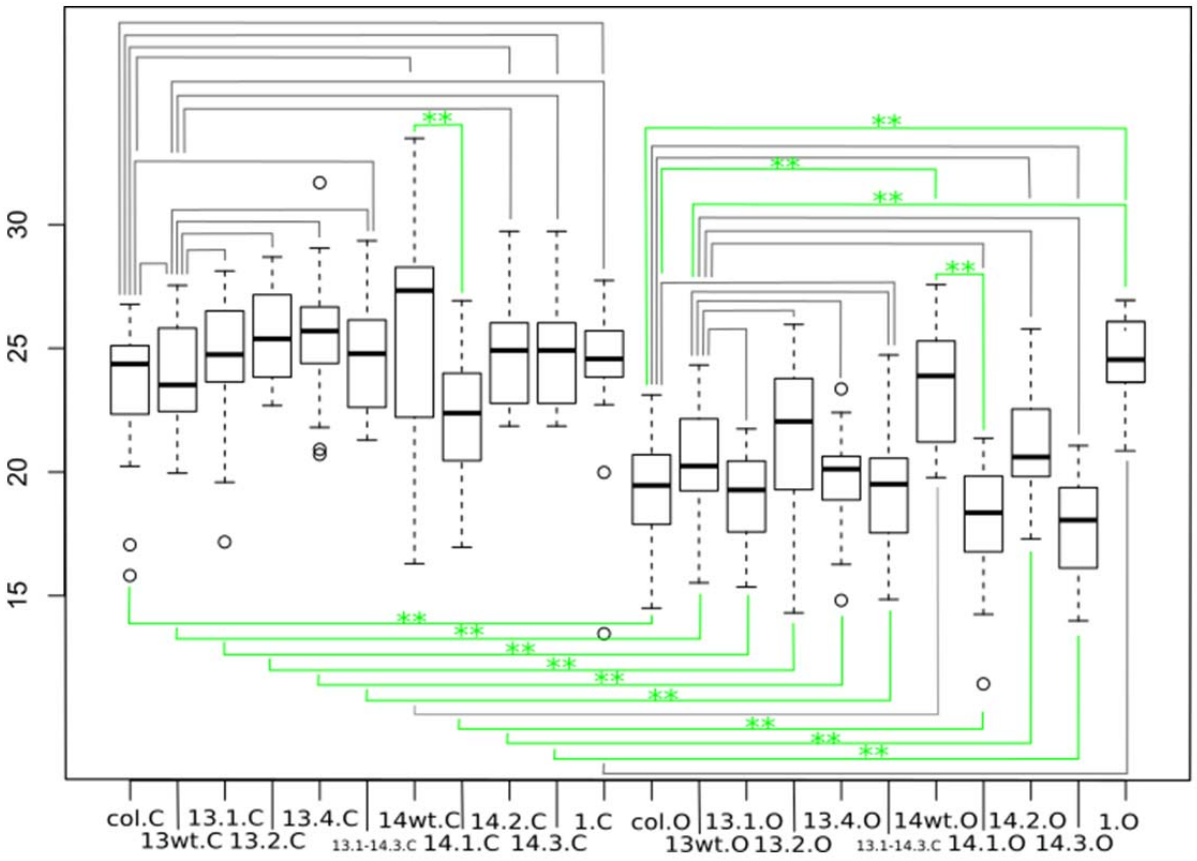

Figure 18. (Q1top half + Q2 bottom half) boxplot graph showing root length of 7DAG seedlings after 3 days on 0,01mM oryzalin treatment (O) and Control media without treatment(C). The relevant combinations of compared genotypes have been marked with a clamp and highlighted with asterisk in case of significance, genotypes compared with wt(upper half of the graph), treated and non-treated plants (lower part). **p<0,01;*p<0,05.

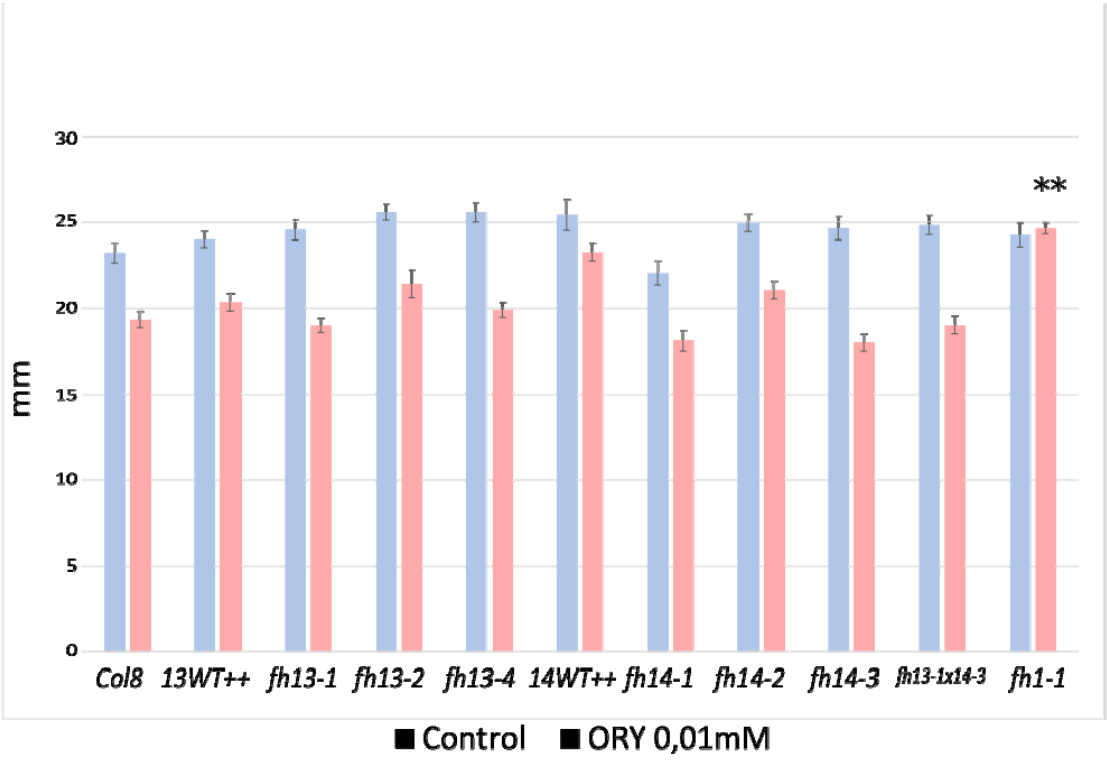

Figure 19. (Q1) Graph showing average root length of 7DAG seedlings after 3 days on 0,01mM oryzalin treatment (O) and Control media without treatment(C). Asterisk highlights differences between genotype and a relevant wtp<0,01;*p<0,05**

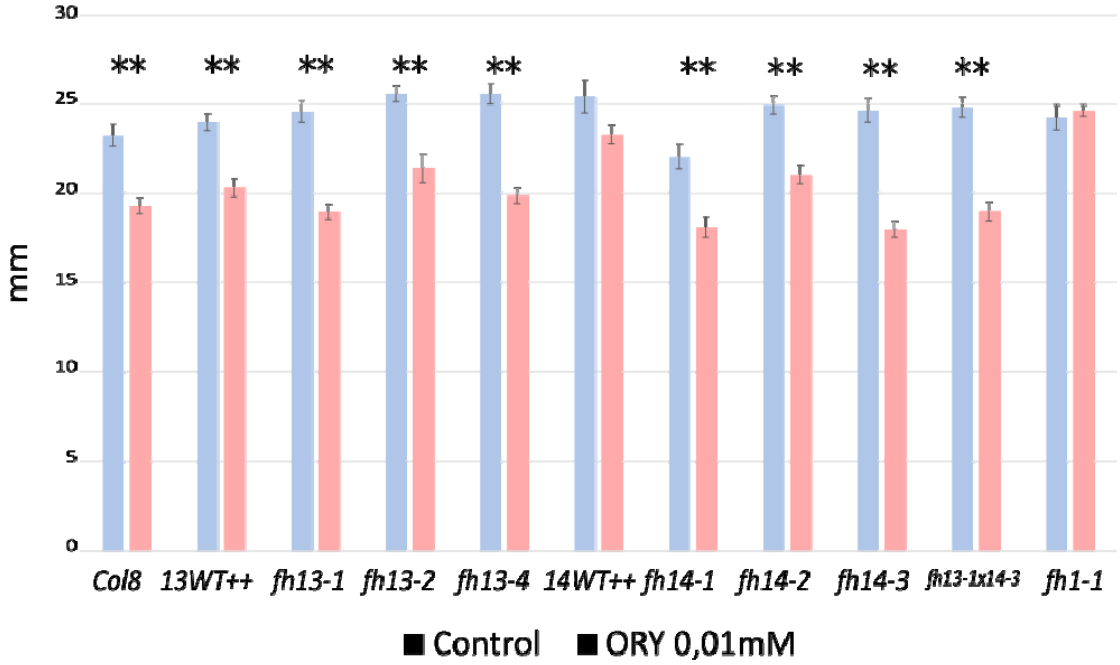

Figure 20. (Q2) Graph showing average root length of 7DAG seedlings after 3 days on 0,01mM oryzalin treatment (O) and Control media without treatment (C). Asterisk highlights significant differences between treated and non-treated plants **p<0,01;*p<0,05

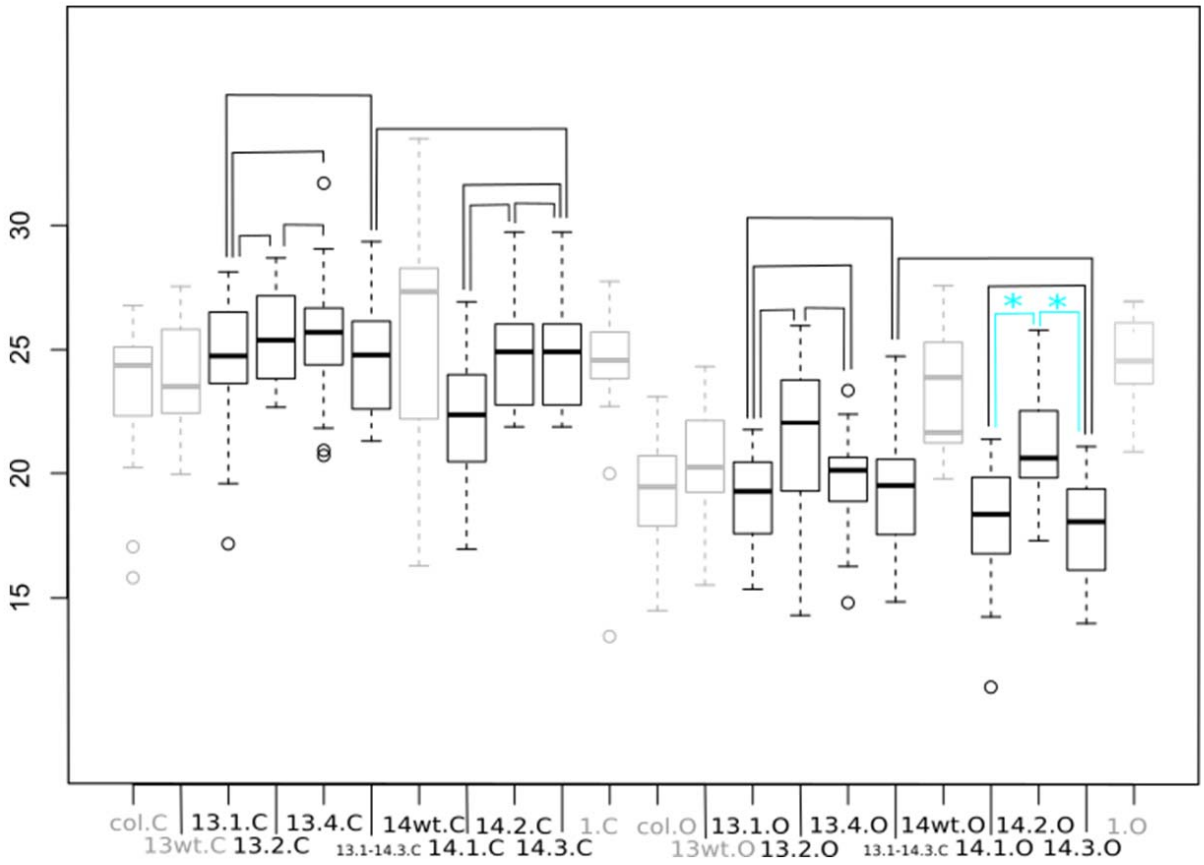

Figure 21. (Q3) boxplot graph showing root length of 7DAG seedlings after 3 days on 0,01mM oryzalin treatment (O) and Control media without treatment (C). Genotypes compared with each other have been marked with a clamp and highlighted with asterisk in case of significance. **p<0,01;*p<0,05

Number of lateral roots

Based on initial qualitative observations, I also investigated effects of formin mutations and inhibitor treatment on root branching. There were trends in increased root number but not all of them could be repeated. Treated and non-treated plants have been compared, which revealed that fh1 is stimulated significantly by latrunculin in production of lateral roots (Figure 23). *fh14*-3 has less lateral roots on latrunculin compared to wt (Figure 22).

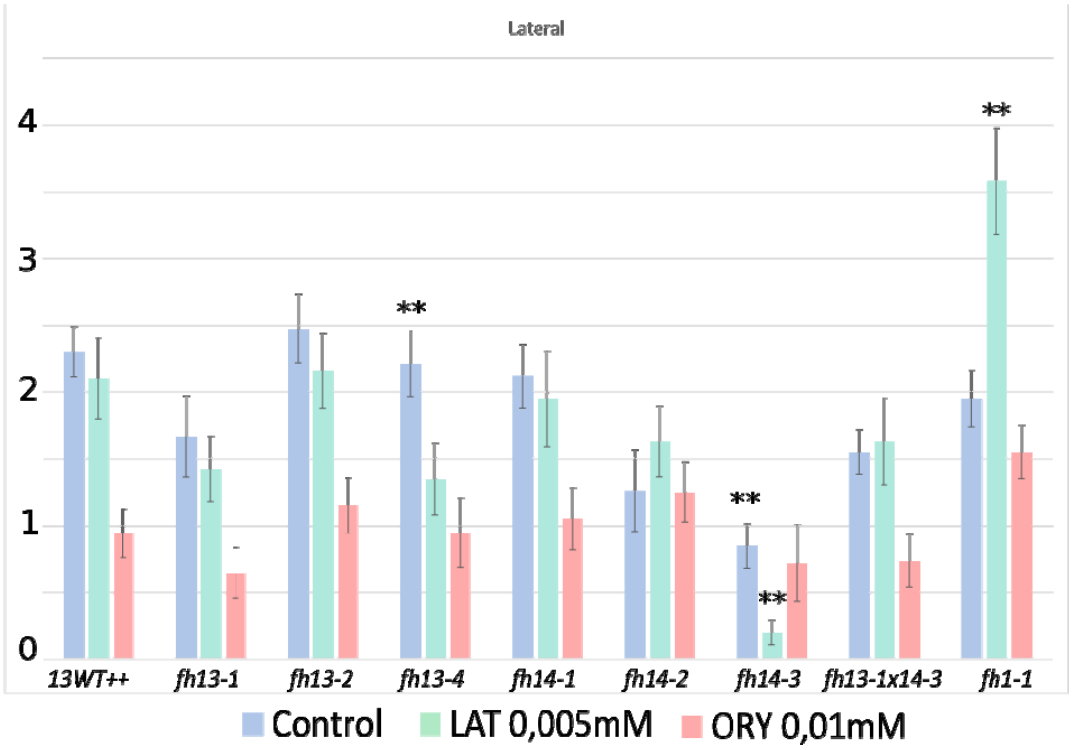

Figure 22. (Q1) Graph showing average number of lateral roots of 7DAG seedlings after 3 days on 0,01mM oryzalin, 0,005mM latrunculin treatment and Control media. Asterisk highlights differences between genotype and a relevant wtp<0,01;*p<0,05 (mind, In this case some lines had significantly altered number of roots, however they were not observed in the following experiment. The only significant alteration that could be repeated was in *fh14-3.*)**

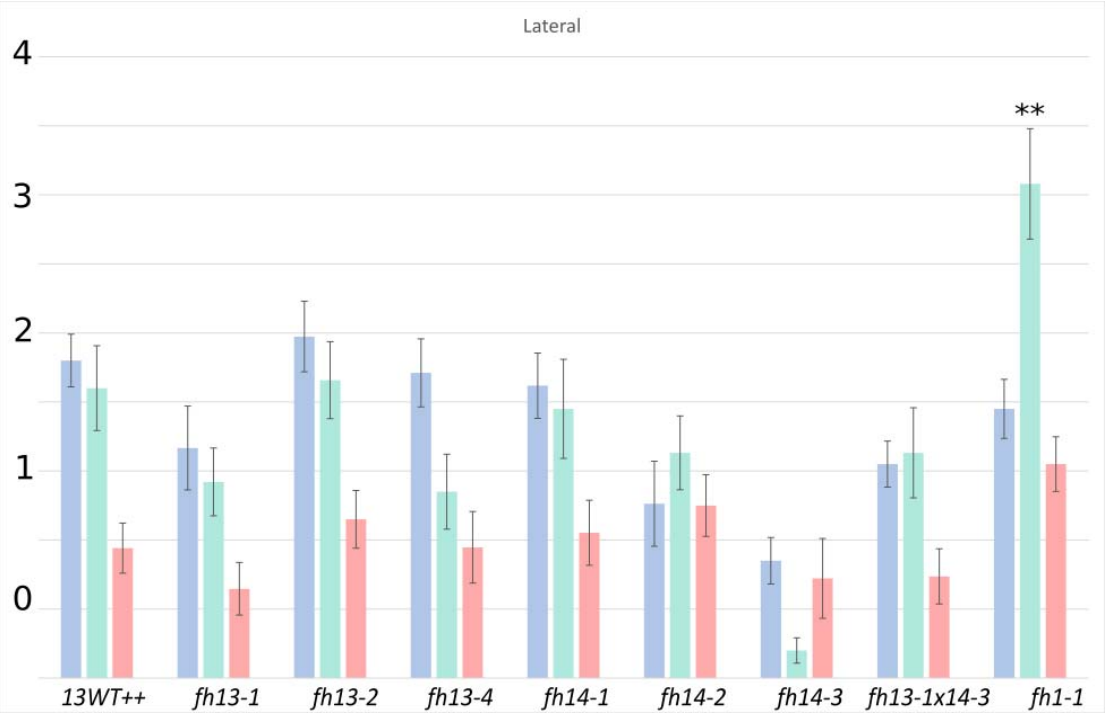

Figure 23. (Q2) Graph showing average number of lateral roots of 7DAG seedlings after 3 days on 0,01mM oryzalin, 0,005mM latrunculin treatment and Control media. Asterisk highlights significant differences between treated and non-treated plants **p<0,01;*p<0,05

Number of adventitious roots

Since seedlings tend to have 0 or 1 adventitious root resulting data was categorical rather than quantitative and had to be processed with an alternative statistical procedure. *fh14-1* had less adventitious roots than Wt when treated with latrunculin (Figure 24.A).

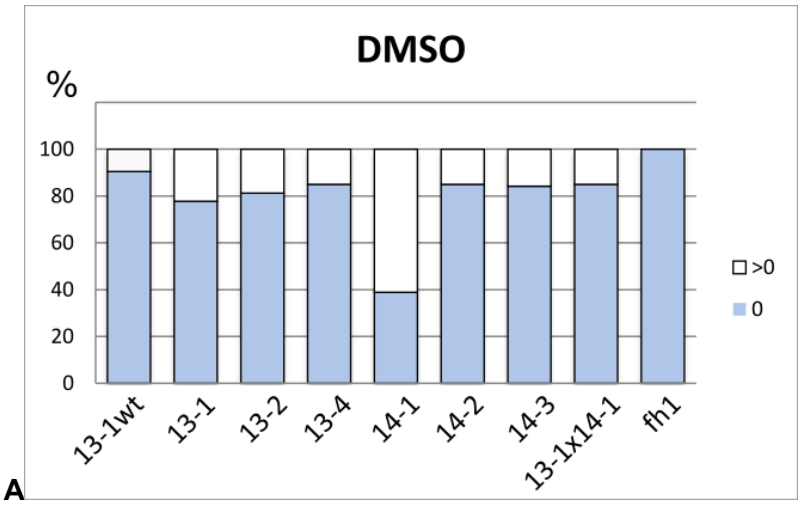

A

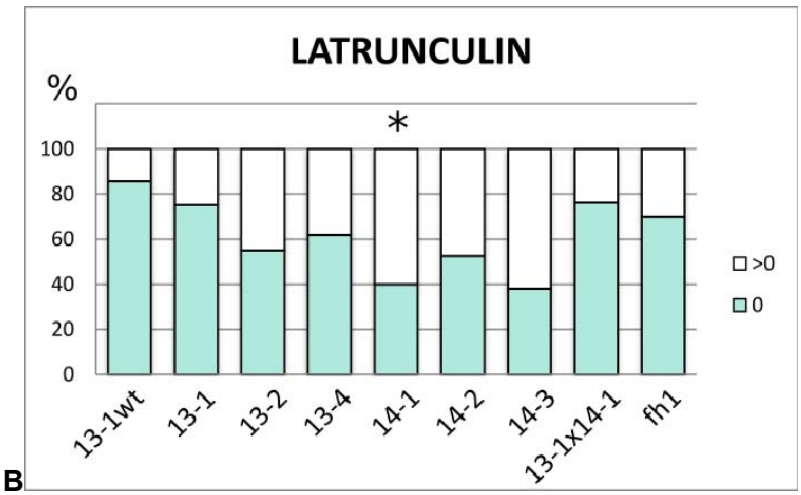

B

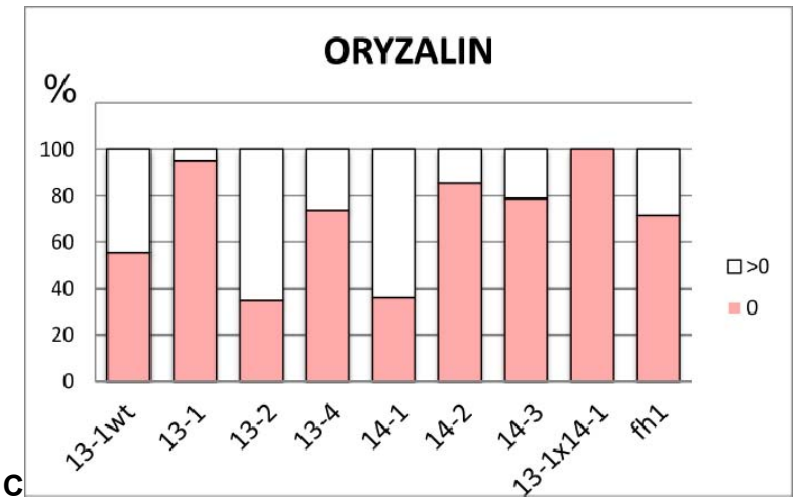

C

Figure 24. Graphs showing number of *plants* with 0 adventitious roots and >0 roots of 7DAG seedlings after 3 days on Control media (A), 0,005mM latrunculin (B) and 0,01mM oryzalin (C). Asterisk highlights significant differences between treated and non-treated plants **p<0,01;*p<0,05. Graph presents lines from *fh13*, *fh14* and *fh1* LOF mutants.

Additional experiments

Evaporation test

Since stomata closure is a dynamic process regulated by the cytoskeleton, we also looked for phenotype during desiccation. An evaporation test has been performed. If *fh13* has a significant influence on cytoskeletal dynamics during stomata closure, we should be able to observe it. *fh13* lines have been compared with wt under same conditions. Another actin nucleator (Beltzner and Pollard, 2004), *arpC5* has been used as a control. *arpC5* (or CRK (Mathur, 2003c)) is known to have slits between epidermal cells and thus is known to be sensitive to drought.

Data has been collected from 3 independent experiments. Though there has been a trend in *fh13*-2 being the most sensitive to drying out it has not been significant in all experiments (Figure 25). Weight loss of *arpC5* was the fastest as expected.

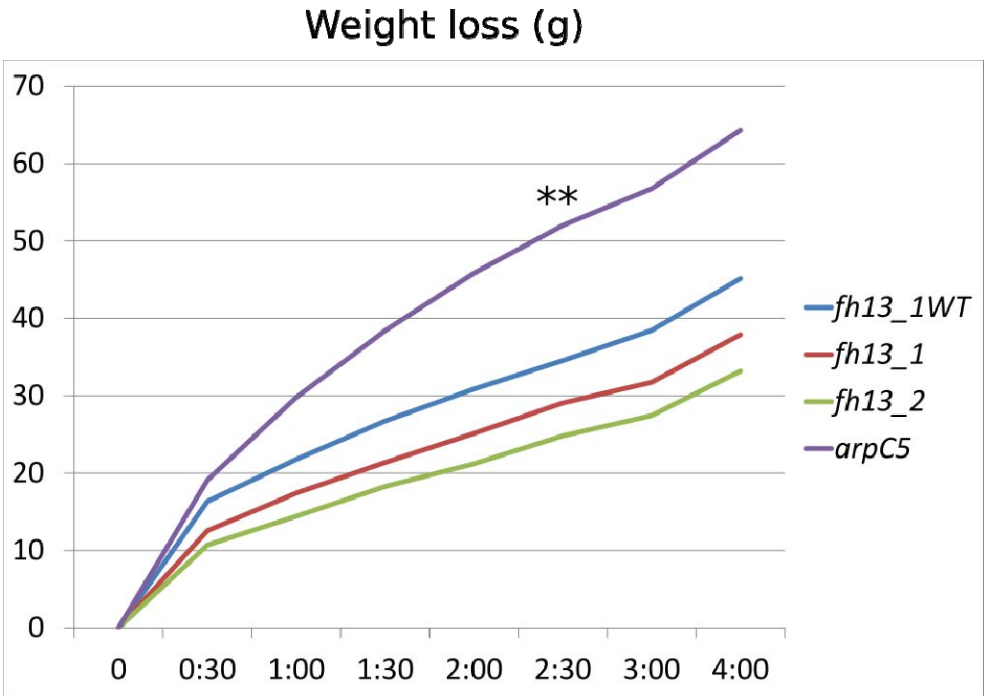

Figure 25. Average weight loss during four hours of measuring leaves of 28 days old plants.

Pavement cell circularity

No significant phenotype has been found in the epidermal cells in terms of area, perimeter or circularity. None of the genotypes altered from wt (Figure 27). However, cells of *fh14*-2 are significantly smaller than *fh14*-3 in perimeter ($p<0,5$) and more circular ($p<0,01$).

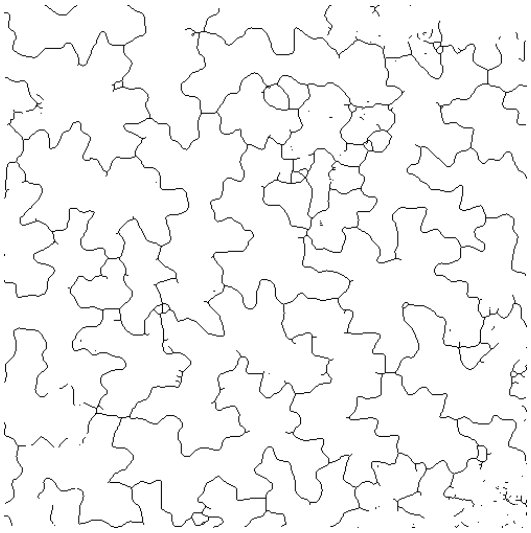

Figure26. An exemplary picture shows a binary image of pavement cells after processing in imageJ ready to be measured.

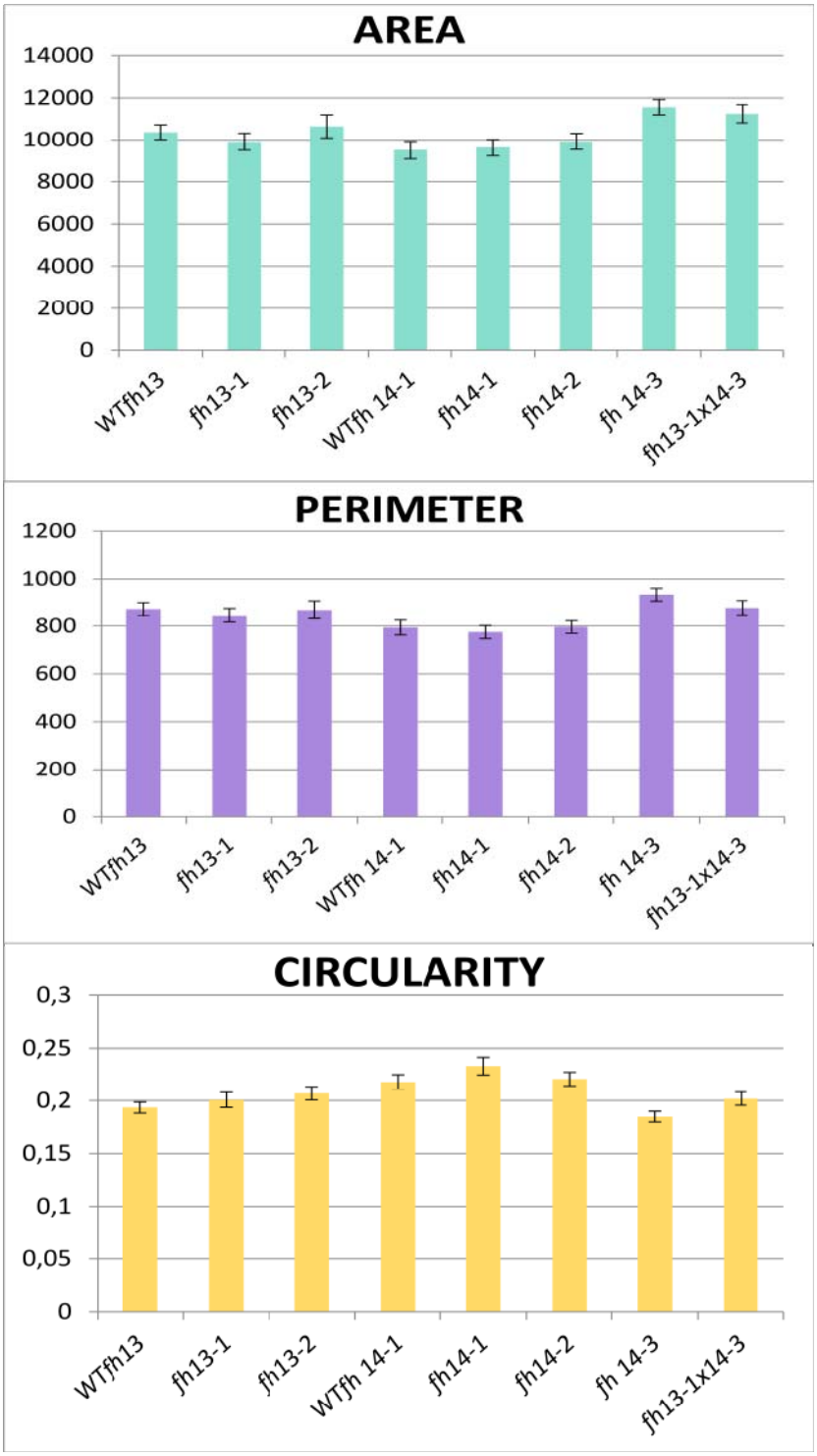

Figure 27. Graphs showing area, perimeter and circularity of epidermal cells of 10DAG seedlings

Results-summary

Main root length

No significant phenotype has been observed in *fh13* and *fh14*. The effect of cytoskeletal drugs on root length of *fh13* and *fh14* was comparable to wt. Cytoskeletal drugs affected wt plants (Figure 16 and Figure 20) thus we can conclude that the treatment was done correctly. *Fh1* resistance to low doses of oryzalin has also been observed (Figure 20).

Lateral branching

On control media *fh14*-3 tends to have less lateral roots than wt, this trend has been enhanced by latrunculin treatment and became statistically relevant (Figure 22). When comparing treated and non-treated plants, we can see no significant influence of cytoskeletal drugs except for *fh1*, interestingly lateral branching is stimulated by latrunculin (Figure 23).

Adventitious branching

Fh14-1 generally tends to have less adventitious roots. Latrunculin enhances this trend and makes it statistically relevant (Figure 24.A). Any other significant alterations in root branching that could be repeated were not found. However, we observed certain trends. Adventitious roots seem to be supressed by oryzalin in *fh13-1, fh14-2, fh14-3* and double mutant (Figure 24B). Latrunculin tends to stimulate adventitious branching mostly in *fh13-2* and *fh14-2* (Figure 24.A).

Double crosses

Crossing *fh13* with *fh14* was efficient. Double mutants also had no obvious phenotype. Though FH2 domains of *fh13* and *fh14* are able to form a heterodimer (Houšková, 2015), the function is not largely affected by losing both genes and quite possibly independent on each other.

Discussion

Root measuring methods – pros and cons

The size of the present project, including large amount of plants, three mutant lines for each gene and their WT, seedlings had to be scanned in gross quantities in shortest time possible. Flatbed scanners operated by MULTISCAN (Slovak *et al.*, 2014) turned out to be excellent tools for imaging. However subsequent BRAT (Slovak *et al.*, 2014) analysis was less sufficient and could not be relied on. I used manual measuring tools in ImageJ. Two-way ANOVA was able to eliminate mistake and handle multiple conditions in experiment.

To gain access to roots, we have used *in vitro* cultivation on agar media. This has several benefits. Firstly, visualisation of root system in soil is complicated and while accessing the roots could be damaged. Secondly, *in vitro* plants are not affected by influences such as bacteria and fungi. Conditions are easier to control and keep constant for each experiment. Third reason is due to visualisation method recently introduced to our laboratory: MULTISCAN and BRAT (Slovak *et al.*, 2014). Thus, size and number of our plants was determined by the size of the scanner blocks. Both scanners and the follow-up program had to be tested in order to catch up with potential problems. In order to improve visualisation of the root system we placed a sheet of black paper on top of the plates while scanning. This created a dark background and enhanced contrast. Although plates were scanned from underneath, water condensation on the plate lid had to be eliminated. A sufficient way is to add more agarose to the media. 1% agarose turned out to be better for scanning.
Size of the plants was adequate up to 10 days, after that BRAT had problems recognizing root system among individual plants. Similar problems were described in alternative program WZ-Rhizo (Armengaud, 2009). For long-term cultivation plants would have to be grown in larger containers such as rhizometers (Judd *et al.*, 2015) with a subsequent analysis program which could measure length, speed of root growth, presence and quantity of root hairs, and root branching/architecture of older plants. Rhizometers eliminate the risk of root damage. Since we have not found major phenotype of our mutant lines treated by cytoskeletal drugs, future observations could

be done on soil-grown plants under other stress conditions such as drought suggested in previous studies (Přerostová, 2011).

Phenotypic analysis of formin mutants

No significant phenotype has been observed in *fh13* and *fh14* on control media, which is consistent with previous observations (Přerostová, 2011). Though *fh14-1* had significantly shorter roots compared with *fh14-1WT++* (Figure18,Figure 19), these results could not be justified due to unexpected insertion in this line. *Fh14-1WT++* itself seems to have a phenotype. Although this has not been documented, the differences were noticeable. A certain number of individuals germinated later, had thicker and shorter stem and seemed to be more resilient to drought. Therefore we cannot sufficiently pair *fh14-1* with an adequate control (see Controls and wild types).

Drug treatment did not reveal mutant phenotype in terms of root length

It has been reported that latrunculin inhibits root growth by 50% to 70% in concentration 17nM. This was due to decreased cell division rather than cell elongation (Rahman *et al.*, 2007). There are studies describing how application of cytoskeletal drugs mimics the effect of other substances or mutations. It has been observed that *fh1* mimics the effect of SMIFH2 to a certain extent (Rosero *et al.*, 2013). However, the range of formin homologues has various functions and by inhibiting their FH2 actin binding domain at once, the cytoskeleton should be affected on much larger scale compared to loss of function of a single formin (Rosero *et al.*, 2016). Latrunculin mimics the effect of disrupted auxin transport by 2,4-dichlorophenoxy-acetic acid (2,4-D) and naphthylphthalamic acid (NPA) in terms of cell division and cytoplasmic streaming (Rahman *et al.*, 2007). However, 2,4-D also affects microtubule polymerization *in vitro* (Rosso *et al.* 2000). Thus, observed phenotypes cannot be simply interpreted as defects in auxin transport. In our study, *fh13* and *athf14* did not mimic the effect of latrunculin or oryzalin treatment on wt.

Sensitivity to actin-targeted drugs has been claimed to be a direct consequence of altered microtubule scaffolding. Experiments with MICROTUBULE ORGANIZATION 1 (MOR1) revealed that *mor*-1 mutant is hypersensitive to latrunculin. Also, plants with defective actin network are hypersensitive to oryzalin. Based on previous studies with FH14, which show that FH14 binds MTs with a higher affinity than to AFs (Li *et al.*,

2010) (see introduction), we could expect that decreasing expression of fh14 should increase sensitivity to latrunculin.

With respect to overall main root length, we observed no hypersensitivity, the effect of cytoskeletal drugs was comparable with wt (Figure 16) and to other mutants (Figure17). Thus, formin function remains a question.

Cross-talk between microfilament and microtubule organization is important for regulating anisotropic cell expansion (Collings *et al.*, 2006).
Nevertheless, among this statement we cannot conclude anything else. Actin network and microtubules are connected indeed, but drug treatment does not reveal details of this cross-talk.

Other formin mutants have been previously reported to be latrunculin sensitive.
Class I formin *fh8* primary root growth and lateral root initiation was inhibited by low doses of latrunculin. Root meristem of fh8 was more sensitive than wt. Fh8 was localized at the nuclear envelope, suggesting a crucial role in cell division (Xue *et al.*, 2011).

In previous studies *fh1* epidermal pavement cells also showed increased sensitivity to latrunculin (Rosero *et al.*, 2016), in terms of root diameter and root growth rate (Rosero *et al.*, 2013). Closer observation of developing root cells in *fh1* x GFP-MAP4 crossbreeds revealed more frequent actin bundles when treated with latrunculin (Rosero *et al.*, 2013).

_Fh13_ and _fh14_ show no changes in resistance to cytoskeletal drugs

Oryzalin had low effect on *fh1* mutant compared to wt suggesting resistance to oryzalin (Rosero *et al.*, 2013). Authors of this study admit possible role of FORMIN1 in actin-tubulin crosstalk (Rosero *et al.*, 2013).

Consistent with this study, in our experiments oryzalin also had low effect on *fh1* mutant compared to wt. No such resistance was found in *fh13* and *fh14*. Combination of cytoskeletal drugs and formin class II mutation was comparable with treated wt.

Drug treatment affects root branching

Interestingly, *fh1* seems to be stimulated by latrunculin in lateral root formation (Figure 23). How can we interpret this phenotype? Plants are able to compensate uptake defects on cellular level by increasing surface on organ level. This could explain why some plants tend to have more developed root system when treated with latrunculin.

Alternative software has previously found that lateral branching is highly variable with a variation coefficient of 130% in contrast to 20% variability in length (Armengaud, 2009). I suggest more experiments should be done in order to confirm our observations. If these observations continue inconsistent, we can blame natural variation and could conclude that FH13 and FH14 mutation has no effect on root development even when treated by cytoskeletal drugs.

Fh14-3 shows decreased number of lateral roots after latrunculin treatment (Figure 22). FH14-3 seems to be involved in lateral root development similarly to FH8 which regulates lateral meristem initiation during cell division (Xue *et al.*, 2011). However fh14-3 could play role in a different mechanism. Lateral root development is mostly regulated by auxin signalling (Dubrovsky *et al.*, 2008). An important player in membrane recycling capabilities of the auxin transporters is phosphatidylinositol-3,5-bisphosphate (Hirano and Sato, 2011). Since PTEN domain of ClassII formins might be able to bind membrane via phosphatidylinositol-3,5-bisphosphate in moss (van Gisbergen *et al.*, 2012), perhaps fh14 also plays role in directing actin transporters to the plasma membrane.

Additional experiments

As an alternative approach towards characterizing the effects of formin mutation, we also tried visualising the cytoskeleton in *fh13* and *fh14* plants in order to elucidate the whole situation in the cell by crossing GFP and YFP-labelled actin as well as GFP-MAP4 mutants with *fh13* and *fh14*. The results were so far unsatisfactory. Fluorescent signal weakened with every generation until it was almost invisible. Similarly, previous study with fh1 revealed resistance to oryzalin, but this ability to compensate has not been explained in detail. Microtubule-stabilizing GFP-MAP4 marker seems to interact with formin mutation in the regulation of microtubule dynamics. While oryzalin and latrunculin increased pavement cell circularity in wt without marker plants, expression

of GFP-MAP4 prevented these changes. Stabilization of microtubules by the marker seems to compensate for the drug effects (Rosero *et al.*, 2016). Thus, we decided to continue observations without fluorescently labelled actin.

As in previous studies we expect formin mutations to disrupt polar growth and cell shape. Similar experiments have been performed with class I formin *fh1* (Rosero *et al.*, 2013). Although SMIFH2 treated plants and *fh1* mutants had subtle effect on cotyledon shape *fh1* (Rosero *et al.*, 2016), in our experiment *fh13* had no significant effect on cell shape, concluding that fh13 does not play crucial role in polarized growth of pavement cells.

I have tested mutant plants on the speed of stomata closure and compactability of epidermis by preforming evaporation test. The results were comparable to wt and thus we conclude that FH13 does not affect stomata and epidermal cell shape on larger scale.

Conclusions

Fh13 and *fh14* lines have been compared with adequate wt in order to characterize mutant phenotype in early root system development. My data show no significant alterations, indicating that FH13 and FH14 have no significant phenotype in terms of root length. However, I developed a reliable method for measuring and analysing root length with relevant statistical methods.

By using small doses of cytoskeletal drugs we revealed, that FH13 and FH14 do not play major role in the control of root growth. *Fh1* has also been included in our experiments and consistent with previous studies, did show resistance to oryzalin. Furthermore, we found that root branching is inhibited by latrunculin in *fh14*-3 line. However, more experiments are necessary to confirm our observations.

Acknowledgements

I thank Eva Kollárová for her infinite patience while introducing me to methods of DNA isolation, genotyping and crossing, plant cultivation *in vitro* and *in vivo* and especially for teaching me a systematic way of documentation. I am very grateful to Yazmín Londeo Ríos for her advice while using scanners, also Radek Bezvoda for IT support and servicing BRAT. Furthermore, I would like to thank Ivan Kulich, Petr Sabol and Marta Čadyová for technical support. Acknowledgements to my genious teacher and supervisor Fatima Cvrčková, her ideas and advice and big thanks to my family for moral support.

References

Armengaud, P. (2009). EZ-Rhizo software: the gateway to root architecture analysis. Plant Signal. Behav. *4*, 139–141.

Armour, W.J., Barton, D.A., Law, A.M.K., and Overall, R.L. (2015). Differential Growth in Periclinal and Anticlinal Walls during Lobe Formation in Arabidopsis Cotyledon Pavement Cells. Plant Cell *27*, 2484–2500.

Bartolini, F., Moseley, J.B., Schmoranzer, J., Cassimeris, L., Goode, B.L., and Gundersen, G.G. (2008). The formin mDia2 stabilizes microtubules independently of its actin nucleation activity. J. Cell Biol. *181*, 523–536.

Beltzner, C.C., and Pollard, T.D. (2004). Identification of Functionally Important Residues of Arp2/3 Complex by Analysis of Homology Models from Diverse Species. J. Mol. Biol. *336*, 551–565.

Blanchoin, L., Amann, K.J., Higgs, H.N., Marchand, J.B., Kaiser, D.A., and Pollard, T.D. (2000). Direct observation of dendritic actin filament networks nucleated by Arp2/3 complex and WASP/Scar proteins. Nature *404*, 1007–1011.

Chang, F. (1997). cdc12p, a Protein Required for Cytokinesis in Fission Yeast, Is a Component of the Cell Division Ring and Interacts with Profilin. J. Cell Biol. *137*, 169–182.

Collings, D.A., Lill, A.W., Himmelspach, R., and Wasteneys, G.O. (2006). Hypersensitivity to cytoskeletal antagonists demonstrates microtubule-microfilament cross-talk in the control of root elongation in Arabidopsis thaliana. New Phytol. *170*, 275–290.

Cvrcková, F., Novotný, M., Pícková, D., and Zárský, V. (2004). Formin homology 2 domains occur in multiple contexts in angiosperms. BMC Genomics *5*, 44.

Cvrčková, F., Grunt, M., Bezvoda, R., Hála, M., Kulich, I., Rawat, A., and Žárský, V. (2012). Evolution of the Land Plant Exocyst Complexes. Front. Plant Sci. *3*.

Deeks, M.J., and Hussey, P.J. (2003). Arp2/3 and “The Shape of things to come.” Curr. Opin. Plant Biol. *6*, 561–567.

Deeks, M.J., Fendrych, M., Smertenko, A., Bell, K.S., Oparka, K., Cvrckova, F., Zarsky, V., and Hussey, P.J. (2010). The plant formin AtFH4 interacts with both actin and microtubules, and contains a newly identified microtubule-binding domain. J. Cell Sci. *123*, 1209–1215.

Dubrovsky, J.G., Sauer, M., Napsucialy-Mendivil, S., Ivanchenko, M.G., Friml, J., Shishkova, S., Celenza, J., and Benkova, E. (2008). Auxin acts as a local morphogenetic trigger to specify lateral root founder cells. Proc. Natl. Acad. Sci. *105*, 8790–8794.

Evangelista, M. (2003). Formins: signaling effectors for assembly and polarization of actin filaments. J. Cell Sci. *116*, 2603–2611.

Favery, B. (2004). Arabidopsis Formin AtFH6 Is a Plasma Membrane-Associated Protein Upregulated in Giant Cells Induced by Parasitic Nematodes. PLANT CELL ONLINE *16*, 2529–2540.

Van Gisbergen, P.A.C., Li, M., Wu, S.-Z., and Bezanilla, M. (2012). Class II formin targeting to the cell cortex by binding PI(3,5)P2 is essential for polarized growth. J. Cell Biol. *198*, 235–250.

Grunt, M., Žárský, V., and Cvrčková, F. (2008). Roots of angiosperm formins: The evolutionary history of plant FH2 domain-containing proteins. BMC Evol. Biol. *8*, 115.

Higgs, H.N. (2005). Formin proteins: a domain-based approach. Trends Biochem. Sci. *30*, 342–353.

Hirano, T., and Sato, M.H. (2011). Arabidopsis *FAB1A/B* is possibly involved in the recycling of auxin transporters. Plant Signal. Behav. *6*, 583–585.

Houšková A. (2015). Identification and characterization of proteins interacting with plant formins Diploma thesis. Charles University in Prague. Submitted 2015.

Judd, L., Jackson, B., and Fonteno, W. (2015). Advancements in Root Growth Measurement Technologies and Observation Capabilities for Container-Grown Plants. Plants *4*, 369–392.

Kato, T., Watanabe, N., Morishima, Y., Fujita, A., Ishizaki, T., and Narumiya, S. (2001). Localization of a mammalian homolog of diaphanous, mDia1, to the mitotic spindle in HeLa cells. J. Cell Sci. *114*, 775–784.

Kovar, D.R. (2006). Molecular details of formin-mediated actin assembly. Curr. Opin. Cell Biol. *18*, 11–17.

Kovar, D.R., Kuhn, J.R., Tichy, A.L., and Pollard, T.D. (2003). The fission yeast cytokinesis formin Cdc12p is a barbed end actin filament capping protein gated by profilin. J. Cell Biol. *161*, 875–887.

Le, J., El-Assal, S.E.-D., Basu, D., Saad, M.E., and Szymanski, D.B. (2003). Requirements for Arabidopsis ATARP2 and ATARP3 during Epidermal Development. Curr. Biol. *13*, 1341–1347.

Lenka Stillerová (2014). Cloning and characterization of selected class II formins. Diploma thesis. Charles University in Prague. Submitted 2014

Lewkowicz, E., Herit, F., Le Clainche, C., Bourdoncle, P., Perez, F., and Niedergang, F. (2008). The microtubule-binding protein CLIP-170 coordinates

mDia1 and actin reorganization during CR3-mediated phagocytosis. J. Cell Biol. *183*, 1287–1298.

Li, J. (1997). PTEN, a Putative Protein Tyrosine Phosphatase Gene Mutated in Human Brain, Breast, and Prostate Cancer. Science *275*, 1943–1947.

Li, F., and Higgs, H.N. (2003). The mouse Formin mDia1 is a potent actin nucleation factor regulated by autoinhibition. Curr. Biol. CB *13*, 1335–1340.

Li, Y., Shen, Y., Cai, C., Zhong, C., Zhu, L., Yuan, M., and Ren, H. (2010). The Type II Arabidopsis Formin14 Interacts with Microtubules and Microfilaments to Regulate Cell Division. Plant Cell *22*, 2710–2726.

Maas, R.L., Zeller, R., Woychik, R.P., Vogt, T.F., and Leder, P. (1990). Disruption of formin-encoding transcripts in two mutant limb deformity alleles. Nature *346*, 853–855.

Maehama, T., and Dixon, J.E. (1998). The Tumor Suppressor, PTEN/MMAC1, Dephosphorylates the Lipid Second Messenger, Phosphatidylinositol 3,4,5-Trisphosphate. J. Biol. Chem. *273*, 13375–13378.

Martinière, A., Gayral, P., Hawes, C., and Runions, J. (2011). Building bridges: formin1 of Arabidopsis forms a connection between the cell wall and the actin cytoskeleton: AtFH1 links the cell wall and actin cytoskeleton. Plant J. *66*, 354–365.

Mathur, J. (2003a). Arabidopsis CROOKED encodes for the smallest subunit of the ARP2/3 complex and controls cell shape by region specific fine F-actin formation. Development *130*, 3137–3146.

Mathur, J. (2003b). Mutations in Actin-Related Proteins 2 and 3 Affect Cell Shape Development in Arabidopsis. PLANT CELL ONLINE *15*, 1632–1645.

Mathur, J. (2003c). Arabidopsis CROOKED encodes for the smallest subunit of the ARP2/3 complex and controls cell shape by region specific fine F-actin formation. Development *130*, 3137–3146.

Michelot, A. (2005). The Formin Homology 1 Domain Modulates the Actin Nucleation and Bundling Activity of Arabidopsis FORMIN1. PLANT CELL ONLINE *17*, 2296–2313.

Michelot, A., Derivery, E., Paterski-Boujemaa, R., Guérin, C., Huang, S., Parcy, F., Staiger, C.J., and Blanchoin, L. (2006). A Novel Mechanism for the Formation of Actin-Filament Bundles by a Nonprocessive Formin. Curr. Biol. *16*, 1924–1930.

Nebenführ, A., Gallagher, L.A., Dunahay, T.G., Frohlick, J.A., Mazurkiewicz, A.M., Meehl, J.B., and Staehelin, L.A. (1999). Stop-and-Go Movements of Plant Golgi Stacks Are Mediated by the Acto-Myosin System. Plant Physiol. *121*, 1127–1141.

Pollard, T.D., and Borisy, G.G. (2003). Cellular Motility Driven by Assembly and Disassembly of Actin Filaments. Cell *112*, 453–465.

Přerostová S. (2011). Charakterizace PTEN domény vybraných forminů II. třídy Arabidopsis. Diploma thesis. Charles University in Prague. Submitted 2011

Pruyne, D. (2002). Role of Formins in Actin Assembly: Nucleation and Barbed-End Association. Science *297*, 612–615.

Rahman, A., Bannigan, A., Sulaman, W., Pechter, P., Blancaflor, E.B., and Baskin, T.I. (2007). Auxin, actin and growth of the Arabidopsis thaliana primary root: Auxin and actin interaction. Plant J. *50*, 514–528.

Robinson, R.C. (2001). Crystal Structure of Arp2/3 Complex. Science *294*, 1679–1684.

Rosales-Nieves, A.E., Johndrow, J.E., Keller, L.C., Magie, C.R., Pinto-Santini, D.M., and Parkhurst, S.M. (2006). Coordination of microtubule and microfilament dynamics by Drosophila Rho1, Spire and Cappuccino. Nat. Cell Biol. *8*, 367–376.

Rosero, A., Zarsky, V., and Cvrckova, F. (2013). AtFH1 formin mutation affects actin filament and microtubule dynamics in Arabidopsis thaliana. J. Exp. Bot. *64*, 585–597.

Rosero, A., Oulehlová, D., Stillerová, L., Schiebertová, P., Grunt, M., Žárský, V., and Cvrčková, F. (2016). Arabidopsis FH1 Formin Affects Cotyledon Pavement Cell Shape by Modulating Cytoskeleton Dynamics. Plant Cell Physiol. *57*, 488–504.

Schindelin, J., Arganda-Carreras, I., Frise, E., Kaynig, V., Longair, M., Pietzsch, T., Preibisch, S., Rueden, C., Saalfeld, S., Schmid, B., et al. (2012). Fiji: an open-source platform for biological-image analysis. Nat. Methods *9*, 676–682.

Slovak, R., Goschl, C., Su, X., Shimotani, K., Shiina, T., and Busch, W. (2014). A Scalable Open-Source Pipeline for Large-Scale Root Phenotyping of Arabidopsis. Plant Cell *26*, 2390–2403.

Sparkes, I., Runions, J., Hawes, C., and Griffing, L. (2009). Movement and Remodeling of the Endoplasmic Reticulum in Nondividing Cells of Tobacco Leaves. Plant Cell *21*, 3937–3949.

Theriot, J.A., and Mitchison, T.J. (1993). The three faces of profilin. Cell *75*, 835–838.

Vidali, L., van Gisbergen, P.A.C., Guerin, C., Franco, P., Li, M., Burkart, G.M., Augustine, R.C., Blanchoin, L., and Bezanilla, M. (2009). Rapid formin-mediated actin-filament elongation is essential for polarized plant cell growth. Proc. Natl. Acad. Sci. *106*, 13341–13346.

Wang, J., Zhang, Y., Wu, J., Meng, L., and Ren, H. (2013). AtFH16, an *Arabidopsis* Type II Formin, Binds and Bundles both Microfilaments and Microtubules, and Preferentially Binds to Microtubules: Functional Characterization of a Type II Formin. J. Integr. Plant Biol. *55*, 1002–1015.

Wen, Y., Eng, C.H., Schmoranzer, J., Cabrera-Poch, N., Morris, E.J.S., Chen, M., Wallar, B.J., Alberts, A.S., and Gundersen, G.G. (2004). EB1 and APC bind to mDia to stabilize microtubules downstream of Rho and promote cell migration. Nat. Cell Biol. *6*, 820–830.

Xu, Y., Moseley, J.B., Sagot, I., Poy, F., Pellman, D., Goode, B.L., and Eck, M.J. (2004). Crystal structures of a Formin Homology-2 domain reveal a tethered dimer architecture. Cell *116*, 711–723.

Xue, X.-H., Guo, C.-Q., Du, F., Lu, Q.-L., Zhang, C.-M., and Ren, H.-Y. (2011). AtFH8 Is Involved in Root Development under Effect of Low-Dose Latrunculin B in Dividing Cells. Mol. Plant *4*, 264–278.

Zhang, S., Liu, C., Wang, J., Ren, Z., Staiger, C.J., and Ren, H. (2016). A Processive Arabidopsis Formin Modulates Actin Filament Dynamics in Association with Profilin. Mol. Plant *9*, 900–910.

Zuniga, A. (2004). Mouse limb deformity mutations disrupt a global control region within the large regulatory landscape required for Gremlin expression. Genes Dev. *18*, 1553–1564.